NUREG/CR-6655, Vol. 2
ORNL/TM-13692/V2

Sensitivity and Uncertainty Analyses Applied to Criticality Safety Validation

Illustrative Applications and Initial Guidance

Prepared by
B. L. Broadhead, C. M. Hopper, and C. V. Parks, ORNL

Oak Ridge National Laboratory

U.S. Nuclear Regulatory Commission
Office of Nuclear Regulatory Research
Washington, DC 20555-0001

AVAILABILITY NOTICE

Availability of Reference Materials Cited in NRC Publications

NRC publications in the NUREG series, NRC regulations, and *Title 10, Energy,* of the *Code of Federal Regulations,* may be purchased from one of the following sources:

1. The Superintendent of Documents
   U.S. Government Printing Office
   P.O. Box 37082
   Washington, DC 20402–9328
   <http://www.access.gpo.gov/su_docs>
   202–512–1800

2. The National Technical Information Service
   Springfield, VA 22161–0002
   <http://www.ntis.gov/ordernow>
   703–487–4650

The NUREG series comprises (1) brochures (NUREG/BR-XXXX), (2) proceedings of conferences (NUREG/CP-XXXX), (3) reports resulting from international agreements (NUREG/IA-XXXX), (4) technical and administrative reports and books [(NUREG-XXXX) or (NUREG/CR-XXXX)], and (5) compilations of legal decisions and orders of the Commission and Atomic and Safety Licensing Boards and of Office Directors' decisions under Section 2.206 of NRC's regulations (NUREG-XXXX).

A single copy of each NRC draft report is available free, to the extent of supply, upon written request as follows:

Address: Office of the Chief Information Officer
Reproduction and Distribution
Services Section
U.S. Nuclear Regulatory Commission
Washington, DC 20555–0001
E–mail: <DISTRIBUTION@nrc.gov>
Facsimile: 301–415–2289

A portion of NRC regulatory and technical information is available at NRC's World Wide Web site:

<http://www.nrc.gov>

All NRC documents released to the public are available for inspection or copying for a fee, in paper, microfiche, or, in some cases, diskette, from the Public Document Room (PDR):

NRC Public Document Room
2120 L Street, N.W., Lower Level
Washington, DC 20555–0001
<http://www.nrc.gov/NRC/PDR/pdr1.htm>
1–800–397–4209 or locally 202–634–3273

Microfiche of most NRC documents made publicly available since January 1981 may be found in the Local Public Document Rooms (LPDRs) located in the vicinity of nuclear power plants. The locations of the LPDRs may be obtained from the PDR (see previous paragraph) or through:

<http://www.nrc.gov/NRC/NUREGS/SR1350/V9/lpdr/html>

Publicly released documents include, to name a few, NUREG-series reports; *Federal Register* notices; applicant, licensee, and vendor documents and correspondence; NRC correspondence and internal memoranda; bulletins and information notices; inspection and investigation reports; licensee event reports; and Commission papers and their attachments.

Documents available from public and special technical libraries include all open literature items, such as books, journal articles, and transactions, *Federal Register* notices, Federal and State legislation, and congressional reports. Such documents as theses, dissertations, foreign reports and translations, and non-NRC conference proceedings may be purchased from their sponsoring organization.

Copies of industry codes and standards used in a substantive manner in the NRC regulatory process are maintained at the NRC Library, Two White Flint North, 11545 Rockville Pike, Rockville, MD 20852–2738. These standards are available in the library for reference use by the public. Codes and standards are usually copyrighted and may be purchased from the originating organization or, if they are American National Standards, from—

American National Standards Institute
11 West 42nd Street
New York, NY 10036–8002
<http://www.ansi.org>
212–642–4900

DISCLAIMER

This report was prepared as an account of work sponsored by an agency of the United States Government. Neither the United States Government nor any agency thereof, nor any of their employees, makes any warranty, expressed or implied, or assumes any legal liability or responsibility for any third party's use, or the results of such use, of any information, apparatus, product, or process disclosed in this report, or represents that its use by such third party would not infringe privately owned rights.

NUREG/CR-6655, Vol. 2
ORNL/TM-13692/V2

Sensitivity and Uncertainty Analyses Applied to Criticality Safety Validation

Illustrative Applications and Initial Guidance

Manuscript Completed: October 1999
Date Published: November 1999

Prepared by
B. L. Broadhead, C. M. Hopper, and C. V. Parks

Oak Ridge National Laboratory
Managed by Lockheed Martin Energy Research Corporation
Oak Ridge, TN 37831-6370

C. W. Nilsen, NRC Project Manager

Prepared for
Division of Systems Analysis and Regulatory Effectiveness
Office of Nuclear Regulatory Research
U.S. Nuclear Regulatory Commission
Washington, DC 20555-0001
NRC Job Code W6479

ABSTRACT

This report presents the application of sensitivity and uncertainty (S/U) analysis methodologies developed in Volume 1 to the code/data validation tasks of a criticality safety computational study. Sensitivity and uncertainty analysis methods were first developed for application to fast reactor studies in the 1970s. This work has revitalized and updated the existing S/U computational capabilities such that they can be used as prototypic modules of the SCALE code system, which contains criticality analysis tools currently in use by criticality safety practitioners. After complete development, simplified tools are expected to be released for general use.

The methods for application of S/U and generalized linear-least-squares methodology (GLLSM) tools to the criticality safety validation procedures were described in Volume 1 of this report. Volume 2 of this report presents the application of these procedures to the validation of criticality safety analyses supporting uranium operations where the enrichments are greater than 5 wt %.

Specifically, the traditional k_{eff} trending analyses are compared with newly developed k_{eff} trending procedures, utilizing the D and c_k coefficients described in Volume 1. These newly developed procedures are applied to a family of postulated systems involving $U(11)O_2$ fuel, with H/X values ranging from 0 to 1000. These analyses produced a series of guidance and recommendations for the general usage of these various techniques. Recommendations for future work are also detailed.

CONTENTS

ABSTRACT iii

LIST OF FIGURES vii

LIST OF TABLES ix

EXECUTIVE SUMMARY xi

ACKNOWLEDGMENTS xv

1 INTRODUCTION 1
1.1 BACKGROUND 2

2 DEVELOPMENT OF CRITICAL EXPERIMENT DATABASE 5
2.1 LEU Systems 5
2.2 CSEWG Benchmarks 5
2.3 PCTR Experiments 9
2.4 HEUMET Systems 11
2.5 Rocky Flats Experiments 12
2.6 Russian Critical Experiments 13
2.7 Other Systems 13
2.8 Tabulation of Calculated-versus-Experimental Results and Uncertainties 14

3 USE OF METHODOLOGY FOR GREATER THAN 5-WT % ENRICHED URANIUM APPLICATIONS 19
3.1 Description of $U(11)O_2$ Systems 19
3.2 Sensitivity and Uncertainty Analyses of the $U(11)O_2$ Systems 19
3.3 Traditional Trending Analysis 25
3.4 Trending Analysis Using D Values 34
3.5 Trending Analysis Using c_k Values 38
3.6 GLLSM Analysis of 11-wt % Systems 43
3.7 Summary of Trending Analyses 45

4 GUIDANCE FOR DETERMINATION OF APPLICABILITY AND ADVANCED TRENDING PROCEDURES 47
4.1 Recommendations on the Use of Trending Procedures 47
4.2 Trending Procedures for c_k and D Parameters 48
4.3 Guidance on Estimating Experimental Uncertainties 48
4.4 Future Developments 49

5 SUMMARY 51

6 REFERENCES 53

LIST OF FIGURES

Figure **Page**

1 Correlation coefficients, c_k, for $U(11)O_2$, H/X = 0 system with 102 benchmark experiments 21

2 Correlation coefficients, c_k, for $U(11)O_2$, H/X = 3 system with 102 benchmark experiments 22

3 Correlation coefficients, c_k, for $U(11)O_2$, H/X = 40 system with 102 benchmark experiments 23

4 Correlation coefficients, c_k, for $U(11)O_2$, H/X = 500 system with 102 benchmark experiments 24

5 D coefficients for $U(11)O_2$, H/X = 0 system with 102 benchmark experiments 26

6 D coefficients for $U(11)O_2$, H/X = 3 system with 102 benchmark experiments 27

7 D coefficients for $U(11)O_2$, H/X = 40 system with 102 benchmark experiments 28

8 D coefficients for $U(11)O_2$, H/X = 500 system with 102 benchmark experiments 29

9 Trend plot for k_{eff} versus energy of average lethargy causing fission (EALF) 30

10 Trend plot for k_{eff} versus energy of average lethargy causing capture (EALC) 31

11 Trend plot for k_{eff} versus hydrogen-to-^{235}U ratio (H/X) 32

12 Trend plot for k_{eff} versus enrichment 33

13 Trend plot for k_{eff} versus D_{sum} value for the $U(11)O_2$ H/X = 3 system 35

14 Trend plot for k_{eff} versus D_{sum} value for the $U(11)O_2$ H/X = 40 system 36

15 Trend plot for k_{eff} versus D_{sum} value for the $U(11)O_2$ H/X = 500 system 37

16 Trend plot for k_{eff} versus c_k value for the $U(11)O_2$ H/X = 0 system 39

17 Trend plot for k_{eff} versus c_k value for the $U(11)O_2$ H/X = 3 system 40

18 Trend plot for k_{eff} versus c_k value for the $U(11)O_2$ H/X = 40 system 41

19 Trend plot for k_{eff} versus c_k value for the $U(11)O_2$ H/X = 500 system 42

20 Plot of convergence in predicted k_{eff} bias, [(e-a)/c], for $U(11)O_2$ systems as a function of number of experimental groups considered 44

LIST OF TABLES

Table **Page**

1 Description of 102 benchmark experiments 6

2 PCTR central region experiments 10

3 Dimensions for Tuballoy- and nickel-reflected spheres 11

4 Spherical models for Rocky Flats H/U = 0.77 experiments 12

5 Spherical models for Rocky Flats H/U = 2.03 experiments 13

6 Benchmark descriptions for ORNL L-8 to L-11 experiments 14

7 Measured-versus-calculated k_{eff} values for 102 critical benchmarks 15

8 Correlation coefficients for the $U(11)O_2$ systems 20

9 Predicted Δk bias and its standard deviation based on traditional trending procedure 25

10 Predicted Δk bias and its standard deviation based on D_{sum} trending procedure 34

11 Predicted Δk bias and its standard deviation based on c_k trending procedure 38

12 Predicted Δk bias and its standard deviation based on GLLSM procedure 45

13 Comparison of predicted Δk bias and the standard deviation of the estimated k_{eff} for various procedures . 46

14 Comparison of predicted USL1 and USL2 values for the various procedures 46

EXECUTIVE SUMMARY

Sensitivity and uncertainty (S/U) analysis and the subsequent application of generalized linear-least-squares methods (GLLSM) were developed in the 1970s primarily for application to fast reactor studies. In the 1980s these techniques were expanded in the area of reactor pressure vessel damage analyses. Recently, interest in the United States has increased in the area of cross-section evaluation, with the recognition that these methods can be used to improve the consistency of the nuclear data with respect to integral nuclear criticality experiments. Volume 1 of this report presented the methodology for application of the S/U and GLLSM techniques to the validation of data used in a criticality safety analysis.

Current generation techniques in criticality safety validation studies typically use trending analyses where the calculated effective neutron multiplication factors (k_{eff}) for sets of benchmark critical experiments are trended against physical and spectral indices, like hydrogen-to-fissile ratio (H/X), energy of average lethargy causing fission (EALF), enrichment, solution concentration, etc., to observe their patterns of variation with measured k_{eff} values (typically 1.00). This trending allows for visual estimates of measured- versus-calculated discrepancies (i.e., biases and associated uncertainties) as a function of these spectral/physical parameters. Under this approach, the set of critical benchmarks must be shown via an expert judgement determination to be "applicable" to the particular application area intended for criticality safety studies.

Thus, a great deal of judgement is often needed in the current validation techniques in order to establish the area of applicability. Each of these traditional trending parameters like H/X and EALF can be useful in establishing *possible* areas of applicability; however, most systems have multiple variables and their simultaneous variation can make a *definite* determination of applicability difficult. The combined variations in H/X, soluble poison concentrations, reflected/unreflected geometry, enrichment, and impurity concentrations are treated poorly by using single- or even multiple-parameter trend curves. Similarly, no method is available to determine if there is sufficient *coverage* for the entire range of the parameter trend curves. For example, given systems with H/X values of 200, 500, 1500, is there coverage of the entire range from 200–1500? If experiments with H/X of 0 and 50 are added, is there adequate coverage from 0–1500? If two of these systems have soluble poison levels of 200 ppm and 500 ppm, is there sufficient coverage for 0–500 ppm levels of poison over the full range of H/X? These are difficult questions, with answers typically derived from expert judgement.

Conversely, the application of S/U techniques allows for a formal estimation of the applicability of each of the critical benchmarks in the set to the application area under consideration. Volume 1 of this report has presented techniques that can be utilized in a formal estimation of applicability using integral parameters based on differences in sensitivity profiles between systems (D) and the correlation coefficients between systems (c_k). The D values are defined as the following:

$$D_n = \sum_{i=1}^{g} \left| S_{nai} - S_{nei} \right|$$

$$D_c = \sum_{i=1}^{g} \left| S_{cai} - S_{cei} \right|$$

$$D_s = \sum_{i=1}^{g} \left| S_{sai} - S_{sei} \right| ,$$

where S is the sensitivity of k_{eff} for the safety application, a, or experimental configuration, e, to $\bar{\nu}$(n) for group i or to the capture (c) or scattering (s), cross sections. These parameters are useful, not only as formal estimations of critical benchmark data applicability, but additionally as trending parameters in the traditional criticality safety data validation approach.

A criterion for determining the appropriate cut-off values of D and c_k for adequate "similarity" has been established. The parameters developed for use in this process are calculated by performing a sensitivity and uncertainty analysis on both the selected experiments and the applications of interest. The complete S/U analysis capability is presently limited to one-dimensional (1-D) and two-dimensional (2-D) models of the systems of interest. Future development work will hopefully eliminate this limitation.

A further development under this current work was the investigation of GLLSM. This methodology is an alternative approach to the traditional trending analysis for the determination of bias and the associated uncertainty. Physically the GLLSM is designed to minimize differences between the measured and calculated values of k_{eff} by predicting data changes based on the entire set of criticals used in the data validation process. The inputs needed for such an analysis are almost identical to the concepts presented thus far: the sensitivity coefficients, the cross-section uncertainties, and the actual calculated and measured k_{eff} values, with the addition of an estimate of the uncertainty in the measured k_{eff} values. The "data changes" that result from the application of the GLLSM can then be used to predict (via interpolation or extrapolation) the biases for *any* application determined to be similar to the benchmark area of applicability.

One of the benefits of the GLLSM approach is that, not only can the bias for a given application be estimated, the cumulative "combination" of critical benchmarks can be used to determine the convergence of the procedure. Questions that can be addressed include: *how many* experiments are needed to verify an application, and *how much* correlation to the application is necessary in order to validate the application area?

In Volume 1, the GLLSM is used to predict *how many* experiments and *how much* correlation between experiments are necessary to validate an application area. In Volume 2, the GLLSM is applied as a data validation tool for comparison with trending analyses using typical characteristic parameters as well as the D and c_k parameters.

This current report presents an illustrative application of both the S/U and GLLSM procedures to the validation of criticality safety studies for facilities processing uranium fuels with enrichments greater than 5 wt % for use in commercial power reactors. In the past, these processing facilities have been limited to enrichments at or below 5 wt %. Hence, much of the critical experiment data correspond to these lower enrichments. As a part of this study, a number of critical experiments in the 5–20-wt % range were identified as having been performed in Russia. A number of these experiments were obtained and documented as a result of this work.

As with any criticality data validation, the goal is to estimate the bias trends for ranges over which the criticality safety calculational studies are to be performed. The usefulness of S/U and GLLSM methods in validation studies is demonstrated by performing a validation of a hypothetical set of application scenarios, which consist of 14 systems, each having $U(11)O_2$ fuel with H/X values varying from 0 to 1000. The 11-wt % enrichment is chosen so the entire range of moderations, including dry, is able to achieve criticality. The data validation included traditional trending analyses, trending analyses with the D and c_k parameters developed in Volume 1, and finally the full GLLSM approach. Volume 2 explores the advantages and disadvantages of each approach and presents guidance for general use of these techniques.

The comparisons among the various trending techniques are quite interesting in that they give very different answers, depending on the particular system being analyzed. The predicted biases for various systems are in some cases up to a factor of 15 different between the various trending techniques. The primary reason for these differences is that various systems "look" very similar from the standpoint of certain parameters, but very different with respect to other parameters. In particular, the H/X and EALF parameters, frequently used in current validation efforts, predict similarity between dry systems with high enrichments (93 wt %) and dry systems with intermediate enrichments (10 wt %), while the c_k and D parameters indicate that these systems are

quite different. The net effect of trending with traditional H/X and EALF parameters is a cancellation of effects (the high-enriched systems underpredict by about 1%, the intermediate-enriched systems overpredict by about 2%), which produce a predicted bias of about 0.5% overprediction for a dry $U(11)O_2$ system. The trending with c_k and D parameters produces an estimated bias of between 1 and 2% overprediction because only the intermediate-enriched systems are predicted to be similar to the dry $U(11)O_2$ system. Although the predicted bias from these applications are all positive, the differences in magnitude are a concern, since the prudent application of trending procedures is very important in criticality validation exercises.

As a result of these observations, the following guidance was developed for the usage of the various trending techniques.

- Traditional trending procedures are acceptable for estimation of the bias and associated uncertainty if about 20 benchmarks with a c_k value of 0.8 or higher are included in the benchmark database. It is further recommended that in using the traditional k_{eff} trending procedures that systems with very different physical characteristics, such as high- versus-low enrichment, poisoned-versus-nonpoisoned, wet-versus-dry, etc., not be included together unless that specific effect is being analyzed.

- The advanced trending analyses with the D and c_k coefficients are recommended if fewer experiments than those recommended above are available. Also the primary motivation behind their use is that widely varying systems can be included in the analysis, hence making the effective extrapolation of the existing data more meaningful. The procedure will allow for automatic collecting of experiments that have similar D and c_k coefficients such that the predicted k_{eff} bias should be valid.

- The GLLSM procedure is recommended if existing experiments with c_k values of 0.8 or higher with respect to the area of application are not available. These experiments, possibly having c_k values 0.2–0.6, are not similar to the application; but they are still relevant. A suite of such experiments can be expected to perform quite well using a GLLSM technique if they are suitably chosen to highlight different aspects of the given application system. Under these conditions, the use of GLLSM for validation is possible, although it may still be desirable to initiate an experimental program to obtain additional data. This procedure also allows for the inclusion of noncritical experiments and non-k_{eff} responses in the validation exercises. Further development is required before these GLLSM techniques can become fully functional in a routine criticality safety validation study.

Additional work is needed to enable full use of these methodologies by the criticality safety practitioner. Of immediate importance is the need to extend the sensitivity analysis methodologies to the realm of three-dimensional Monte Carlo codes typically used in criticality safety analysis. Improved sensitivity information can also be obtained by including the effects of the problem-specific cross-section processing. Additional applications need to be explored to gain further confidence in the guidance developed herein and aid in the development of standard processes that can be more easily implemented and applied by criticality safety analysts. Methods to enable full implementation of GLLSM need particular attention. Finally, cross-section uncertainty information is currently rather limited and the need exists to obtain uncertainty data for a number of nuclides important to criticality safety.

ACKNOWLEDGMENTS

This work was supported by the U.S. Nuclear Regulatory Commission under Project JCN W6479, "Development and Applicability of Criticality Safety Software for Licensing Review." The direction of C. W. Nilsen, the NRC project manager, along with D. R. Damon, S. A. Parra and K. J. Hardin, the NRC technical monitors, is acknowledged.

The technical work described in the report has been presented to several audiences and the reports have been reviewed by individuals with a wide spectrum of interests and experience. This process has been valuable to the authors and appreciation to those willing to provide opinions and feedback is gratefully appreciated. In particular the authors would like to recognize the efforts of D. R. Damon and S. A. Parra who provided review comments for the NRC. Useful discussions and technical reviews were also received from R. M. Westfall, W. C. Jordan, and J. F. Mincey of ORNL. The initial suggestions from J. J. Wagschal of the Hebrew University, Jerusalem, relative to presenting the methodology as well as his careful review of the final report were of great benefit to the authors. Similarly the comments and suggestions provided by R. L. Murray of N. C. State University, M. L. Williams of Louisiana State University, R. E. Wilson of Safe Sites of Colorado, Keyes Niemer of Duke Engineering and Services, and F. Trumble of Westinghouse Safety Management Systems helped the authors identify areas where improved clarity and explanation were needed.

1 INTRODUCTION

Sensitivity and uncertainty (S/U) analysis and the subsequent application of generalized linear-least-squares methods (GLLSM) were developed in the 1970s, primarily for application to fast reactor studies.[1,2] In the 1980s they were expanded in the area of reactor pressure vessel damage analyses.[3] Recently interest in the United States has increased in the area of cross-section evaluation with the recognition that these methods can be used to improve the consistency of the nuclear data with respect to some non-criticality integral experiments.[4]

Current-generation techniques in criticality safety validation studies[5] use trending analyses where the calculated effective neutron multiplication factors (k_{eff}) values for sets of benchmark critical experiments are trended against physical and spectral indices, like hydrogen-to-fissile ratio (H/X), energy of average lethargy causing fission (EALF), enrichment, or solution concentration. This trending allows for visual estimates of measured-versus-calculated discrepancies (i.e., biases) as a function of these spectral/physical parameters. Under this approach, a set of critical benchmarks must be shown via an expert judgement determination to be "applicable" to the particular application area intended for criticality safety studies.

Conversely, the application of S/U techniques allows for a formal determination of the applicability of each of the critical benchmarks in the set to the application area under consideration. Volume 1 of this report has presented techniques that can be utilized in a formal determination of applicability using integral parameters based on differences in sensitivity profiles between systems (D) and the correlation coefficients between systems (c_k). These D values are defined as the following:

$$D_n = \sum_{i=1}^{g} \left| S_{nai} - S_{nei} \right|$$

$$D_c = \sum_{i=1}^{g} \left| S_{cai} - S_{cei} \right|$$

$$D_s = \sum_{i=1}^{g} \left| S_{sai} - S_{sei} \right| ,$$

where S is the sensitivity of k_{eff} for the safety application, a, or experimental configuration, e, to $\bar{\nu}$(n) for group i or to the capture (c) or scattering (s) cross sections. These parameters are useful, not only as formal determinations of critical benchmark data applicability, but additionally as trending parameters in the traditional criticality safety data validation approach.

The results from such a S/U analysis can also be directly incorporated into a full GLLSM procedure quite readily, in that only additional information on the measurement uncertainties need be added to perform the analyses. The GLLSM approach described in Volume 1 of this report[6] was used as a research tool to understand the systematics of the D and c_k parameters previously mentioned. These GLLSM results of Volume 1 supported definition of general ranges in the D and c_k parameters which indicate applicability. Based on these studies, systems with c_k values of 0.80 and higher, the sum of the D values less than 1.2, and individual D values of 0.40 and lower, can be used to designate similar systems. The use of the GLLSM procedures in a criticality safety data validation exercise has the advantage of reducing the underlying uncertainties in the criticality safety limits, which can allow for enhanced operational flexibility with little or no safety implications. Additionally, application of the GLLSM procedure should allow for the inclusion of non-k_{eff} responses (e.g., reaction rates) and even noncritical (e.g., subcritical and dosimetry) experimental data into the data validation procedure.

This current report presents an application of both the S/U and GLLSM procedures to the validation of criticality safety studies for facilities processing uranium fuels with enrichments greater than 5 wt % for use in commercial power reactors. In the past, these processing facilities have been limited to enrichments at or below 5 wt %. Hence, much of the critical experiment data correspond to these lower enrichments. As a part of this study, a number of critical experiments in the 5–20-wt % range were identified as having been performed in Russia.[7] Several of these experiments were obtained and documented as a result of this work.[8] The advantage of having these data available is so that the effect of inclusion or exclusion of these data from the benchmark database can be studied.

As with any criticality data validation, the goal is to estimate the bias and associated uncertainty for ranges over which the criticality safety calculational studies are to be performed. The use of S/U and GLLSM methods in these validations studies will be demonstrated herein by performing a validation for a hypothetical set of application scenarios, which consist of 14 systems, each having $U(11)O_2$ fuel with H/X values varying from 0 to 1000. The 11-wt % enrichment is chosen so the entire range of moderations, including dry, is able to achieve criticality. The data validation will be performed using both the traditional trending analyses, trending analysis with the D and c_k parameters, and finally the full GLLSM approach. Advantages and disadvantages of each approach will be explored. Guidance for general use of these techniques will then be given.

The database of 102 critical benchmark experiments used in this study will be described in Section 2. The application of the S/U and GLLSM techniques to the data validation of the hypothetical 11-wt % systems will be discussed in Section 3. Finally, guidance on the general application of these techniques to other situations will be presented in Section 4.

1.1 BACKGROUND

This volume applies a series of newly developed data validation techniques to criticality safety applications. Before launching into the specific analyses, a summary of a current approach is needed. Certainly there are many possible approaches, but the approach briefly described herein is representative of those currently in use at Oak Ridge National Laboratory.[5]

The data validation exercises are most appropriately named trending analyses, since the calculated values of k_{eff} for a set of benchmark critical experiments are plotted against a single parameter, x, typically H/X, EALF, leakage, concentration, etc., to determine a linear fit of k_{eff} with respect to that parameter. The entire set of calculated k_{eff} values is then averaged, and a "pooled" standard deviation, σ_p, (the standard deviation of the entire data set about the average) determined. A bias, $\beta(x)$, is then determined as the difference between the linear fit and the measured k_{eff} value. The bias is a function of the x parameter since the linear fit to k_{eff} can and typically does have a non-zero slope. An uncertainty in this predicted bias is assumed to be the uncertainty in the pooled data times a statistical multiplier, F. In terms of these quantities two upper subcritical limit (USL) parameters are defined:

$$USL1(x) = 1 - \Delta k_m - F_1 \sigma_p + \beta(x), \text{ or alternately}$$

$$USL2(x) = 1 - F_2 \sigma_p + \beta(x),$$

where Δk_m is an additional margin to ensure subcriticality, and F_2 is a more stringent multiplier than F_1. If the analysis finds $\beta(x)$ to be positive at any point in the trending, the methodology of Ref. 5 sets $\beta(x) = 0$ such that no credit is provided for a positive bias (over prediction of k_{eff}).

This work has applied these currently used validation methods, but replaced the standard parameters with the D and c_k values developed in Volume 1 of this report. These techniques combine the validation and determination of areas of applicability tasks, since the D and c_k parameters are utilized for both operations. Similarly, the results from an application of the GLLSM tools to a data validation problem is simply a prediction of the bias and its uncertainty, which can also be utilized in the safety analysis procedures described above.

2 DEVELOPMENT OF CRITICAL EXPERIMENT DATABASE

The key to any criticality safety data validation procedure is the generation of a database of critical benchmark experiments that typically covers a broad range of systems that are in some way similar to the particular application(s) of interest. Several studies[5, 7–10] have reported the generation of large databases of critical experiments and corresponding code input. The inputs for the benchmark experiments are typically generated corresponding to a three-dimensional (3-D) geometry model. Currently, only 1-D and 2-D sensitivity tools are available, which necessitates the conversion of many of these inputs to 1-D or 2-D models. The impact of the revised models on the sensitivities is expected to be small, based on selected studies of this effect.

This section will briefly describe each of the 102 critical benchmark systems included in this analysis. In each case a summary of the problem materials and dimensions will be given, along with a description of the calculation procedures followed. These problems can be broken into several groups, which include: 14 low-enriched uranium (LEU) oxide or fluoride systems with 2–5-wt % uranium fuel and paraffin or stereotex moderators, 14 Cross-Section Evaluation Working Group (CSEWG) data testing benchmarks (a full range of enrichments from about 1 to 93 wt %, dry to fully moderated), the 11 Physical Constants Testing Reactor (PCTR) k_∞ experiments on 2-wt % uranium fuel, 9 high-enriched uranium metal experiments (HEUMET), 8 low-H/X Rocky Flats experiments (RF low H/X) with uranium enrichments of 4.5 wt %, 36 Russian experiments, which consist of various configurations of solution tanks and fuel rod arrays with ^{235}U enrichments ranging from 5 to 89 wt %, and 10 various experiments that include HISS, UH3, and LXX configurations. The complete list of experiments, their enrichments, H/X values, and a brief description are given in Table 1. The following sections give more detailed information on each system.

2.1 LEU Systems

This group of experiments consists of 2–5-wt % uranium oxide and fluoride systems. The UF_4-paraffin systems (experiments Nos. 1–8 in Table 1) are 2- and 3-wt % uranium systems. The critical dimensions for the unreflected homogeneous spherical systems are radii of 44.91, 38.50, 36.38 36.36, 37.67, 49.65, 36.64 and 28.78 cm, respectively.[11] Even though these systems were cuboid systems, the critical spherical dimensions were obtained from Ref. 11 and were converted from measured critical bucklings and extrapolation distances. A total of six experiments with $U(5)_3O_8$ and stereotex were also analyzed (experiment Nos. 9–14 in Table 1). These six criticals were modeled as homogeneous spheres with radii of 35.57, 33.82, 32.17, 32.94, 33.55, and 41.05 cm, respectively.[12] These radii differ slightly from the estimates reported in Ref. 12; however, they were obtained by buckling conversions based on the reported actual critical dimensions and extrapolation distances.

2.2 CSEWG Benchmarks

This group of experiments (15–19, 30–34, 46–48, and 51–52 of Table 1) consists of a number of benchmarks developed over a number of years by CSEWG. These benchmarks are documented in the CSEWG benchmark book;[13] however, they will be described briefly here. GODIVA is a 93-wt %-enriched bare metal sphere with radius of 8.741 cm, and a measured eigenvalue of 1.00 ± 0.003. Big-10 is a cylindrical system consisting of a uranium-metal core, averaging 10 wt % ^{235}U, reflected by depleted-uranium metal. The core has an homogeneous axial region surrounded by interleaved plates of high-enriched uranium and natural uranium such that the average ^{235}U content is uniform. An equivalent spherical system was modeled with a core radius of 30.48 cm and a reflector radius of 45.72 cm. The uncertainty in the measured value of k_{eff} is approximately ±0.003. The ZPR 3.11 assembly is a U(14) metal and steel assembly with a depleted uranium (DU) metal and steel reflector.

Table 1 Description of 102 benchmark experiments

Exp. No.	Enrichment (wt %)	H/X	Application description	Ref.
1	2	195	u(2)f4-ch2 h/x = 195	11
2	2	294	u(2)f4-ch2 h/x = 294	11
3	2	406	u(2)f4-ch2 h/x = 406	11
4	2	496	u(2)f4-ch2 h/x = 496	11
5	2	614	u(2)f4-ch2 h/x = 614	11
6	2	972	u(2)f4-ch2 h/x = 972	11
7	3	133	u(3)f4-ch2 h/x = 133	11
8	3	277	u(3)f4-ch2 h/x = 277	11
9	5	147	u(5)3o8-h2o h/x = 147	12
10	5	245	u(5)3o8-h2o h/x = 245	12
11	5	320	u(5)3o8-h2o h/x = 320	12
12	5	396	u(5)3o8-h2o h/x = 396	12
13	5	503	u(5)3o8-h2o h/x = 503	12
14	5	757	u(5)3o8-h2o h/x = 757	12
15	93	0	godiva-u(93)	13
16	1.3	306	bapl-1 u(1.3) lattice h/x = 306	13
17	1.3	382	bapl-2 u(1.3) lattice h/x = 382	13
18	1.3	515	bapl-3 u(1.3) lattice h/x = 515	13
19	10	0	big-10 u(n)-refl	13
20	93	0	hiss(hug) u(93)-c-b c/x = 303	19
21	98	0	u(98) h2o-refl	15
22	93	0	u(93) 2-u(n)-refl	15
23	93	0	u(93) 3-u(n)-refl	15
24	93	0	u(93) 4-u(n)-refl	15
25	93	0	u(93) 5-u(n)-refl	15
26	93	0	u(93) 7-u(n)-refl	15
27	93	0	u(93) 8-u(n)-refl	15
28	93	0	u(93) 11-u(n)-refl	15
29	93	0	u(93) 8-ni-refl	15
30	93	1378	ornl-1 u(93)o2(no3)2-h2o h/x = 1378	13
31	93	1177	ornl-2 u(93)o2(no3)2-h2o-b h/x = 1177	13
32	93	1033	ornl-3 u(93)o2(no3)2-h2o-b h/x = 1033	13
33	93	972	ornl-4 u(93)o2(no3)2-h2o-b h/x = 972	13

Table 1 (continued)

Exp. No.	Enrichment (wt %)	H/X	Application description	Ref.
34	93	1835	ornl-10 u(93)o2(no3)2-h2o h/x = 1835	13
35	1.157	322	pctr 1.157% 3.73 h/x = 322	14
36	1.071	353	pctr 1.071% 3.78 h/x = 353	14
37	1.006	381	pctr 1.006% 3.83 h/x = 381	14
38	1.071	545	pctr 1.071% 5.84 h/x = 545	14
39	1.157	518	pctr 1.157% 5.99 h/x = 518	14
40	1.006	619	pctr 1.006% 6.23 h/x = 619	14
41	1.157	619	pctr 1.157% 6.90 h/x = 619	14
42	1.006	596	pctr 1.006% 6.95 h/x = 596	14
43	1.071	667	pctr 1.071% 7.14 h/x = 667	14
44	1.006	748	pctr 1.006% 7.52 h/x = 748	14
45	1.157	650	pctr 1.157% 7.52 h/x = 650	14
46	14	0	zpr-3/11 u(14)-fe-ni-cr-mn u(d)-refl	13
47	21	0	zpr-3/12 u(21)-c u(d)-refl	13
48	16	0	zpr-6/6a u(16)-na-fe u(d)-refl	13
49	93	0	uh3 ni-refl	18
50	93	0	uh3 u(n)-refl	18
51	1.3	251	trx-1 u(1.3) lattice h/x = 251	13
52	1.3	429	trx-2 u(1.3) lattice h/x = 429	13
53	93	76	l7 u(93)o2f2-h2o h2o-refl h/x = 76	20
54	93	1110	l8 u(93)o2f2-h2o h/x = 1110	20
55	93	1390	l9 u(93)o2f2-h2o h/x = 1390	20
56	93	126	l10 u(93)o2f2-h2o h2o-refl h/x = 126	20
57	93	1270	l11 u(93)o2f2-h2o h2o-refl h/x = 1270	20
58	5	405	sheba 2 u(5)o2f2-h2o h/x = 405	15
59	4.5	17	rfc 4.5% h/u=.77 met h/x = 17	16
60	4.5	17	rfc 4.5% h/u=.77 met h/x = 17	16
61	4.5	17	rfc 4.5% h/u=.77 met h/x = 17	16
62	4.5	17	rfc 4.5% h/u=.77 met h/x = 17	16
63	4.5	70.7	rf 4.5% h/u=2.03 h/x = 70.7	17
64	4.5	120.1	rf 4.5% h/u=2.03 h/x = 120.1	17
65	4.5	45	rf 4.5% h/u=2.03 h/x = 45	17
66	4.5	45	rf 4.5% h/u=2.03 h/x = 45	17
67	89	92	U(89)o2(no3)2 abrod p = 0	7, 8
68	89	92	U(89)o2(no3)2 abrod p = 6	7, 8
69	89	92	U(89)o2(no3)2 abrod p = 7	7, 8

Table 1 (continued)

Exp. No.	Enrichment (wt %)	H/X	Application description	Ref.
70	89	92	U(89)o2(no3)2 abrod p = 10.57	7, 8
71	89	92	U(89)o2(no3)2 abrod p = 12.3	7, 8
72	89	92	U(89)o2(no3)2 abrod p = 14	7, 8
73	89	92	U(89)o2(no3)2 abrod p = 16	7, 8
74	89	375	U(89)o2(no3)2 76 g/l 0 abrods	7, 8
75	89	375	U(89)o2(no3)2 76 g/l 3 abrods	7, 8
76	89	375	U(89)o2(no3)2 76 g/l 4 abrods	7, 8
77	89	92	U(89)o2(no3)2 289 g/l 0 abrods	7, 8
78	89	92	U(89)o2(no3)2 289 g/l 3 abrods	7, 8
79	89	92	U(89)o2(no3)2 289 g/l 4 abrods	7, 8
80	89	92	U(89)o2(no3)2 289 g/l 6 abrods	7, 8
81	89	92	U(89)o2(no3)2 289 g/l 18 p = 4 rods	7, 8
82	89	92	U(89)o2(no3)2 289 g/l 36 p = 4 rods	7, 8
83	89	92	U(89)o2(no3)2 289 g/l 18 p = 6 rods	7, 8
84	89	92	U(89)o2(no3)2 289 g/l 36 p = 6 rods	7, 8
85	17	628	U(17)o2 34 rods 22.7 C	7, 8
86	17	628	U(17)o2 34 rods 218 C	7, 8
87	17	611	U(17)o2 74 rods 16 C	7, 8
88	17	611	U(17)o2 74 rods 151 C	7, 8
89	17	565	U(17)o2 68 rods 15 C	7, 8
90	17	565	U(17)o2 68 rods 151 C	7, 8
91	10	50	U(10)o2 p = 0.7 20 C	7, 8
92	10	50	U(10)o2 p = 0.7 166 C	7, 8
93	10	50	U(10)o2 p = 0.7 263 C	7, 8
94	10	340	U(10)o2 p = 1.4 20 C	7, 8
95	10	340	U(10)o2 p = 1.4 206 C	7, 8
96	10	340	U(10)o2 p = 1.4 274 C	7, 8
97	10	629	U(10)o2 p = 1.852 20C	7, 8
98	10	629	U(10)o2 p = 1.852 193 C	7, 8
99	10	629	U(10)o2 p = 1.852 263 C	7, 8
100	5.64	973	U(5.64)o2(no3)2 400 g/l 0 rods	7, 8
101	5.64	973	U(5.64)o2(no3)2 400 g/l 1 rod	7, 8
102	5.64	973	U(5.64)o2(no3)2 400 g/l 7 rods	7, 8

The specifications in the CSEWG benchmark book gave a homogeneous spherical model with core radius of 31.61 cm and a 30-cm-thick reflector, with a reported eigenvalue of 1.0000 ± 0.0025. ZPR 3.12 is a U(25) metal, graphite, and steel assembly with a DU metal and steel blanket. The system was modeled as specified in Ref. 13 as homogeneous concentric spheres with radii of 28.76 and 59.26 cm, respectively. The measured value of k_{eff} was reported as 1.0000 with no uncertainty quoted. An uncertainty in k_{eff} due to the use of a 1-D model was specified to be 0.0023. The final ZPR-type assembly included in this analysis was the ZPR 6.6a, which is a large 16 wt %-enriched uranium oxide, sodium and steel core with a DU and steel blanket. A 1-D homogeneous spherical model is specified that consists of core radius and blanket thicknesses of 95.67 and 33.81 cm, respectively. The measured eigenvalue was 1.0000 ± 0.0005, with an estimated 0.05% uncertainty due to the spherical model.

The experiments labeled BAPL-1, -2 and -3 (experiments 16–18 in Table 1) are a series of experiments consisting of a lattice of water-moderated $U(1.3)O_2$ fuel pins in a triangular pitch. The fuel pins for each experiment are identical and have pellet, gap and clad radii of 0.4864, 0.5042, and 0.5753 cm, respectively. The respective pin pitches are 1.5578, 1.6523 and 1.8057 cm for BAPL-1, -2, and -3. These specifications were used to perform cell-weighting calculations with the resulting cell-weighted cross sections input into a 1-D cylindrical model with core and reflector dimensions of 38.1269 and 59.0 cm for BAPL-1, 36.3428 and 56.0 cm for BAPL-2, and 37.6250 and 58.0 cm for BAPL-3. The respective heights for buckling were 137.245, 129.697, and 125.535 cm. No uncertainties on the measured eigenvalues were reported.

The next family of CSEWG critical experiment benchmarks corresponds to the ORNL spheres: ORNL-1, -2, -3, -4, and -10 (experiments 30–34 of Table 1). These unreflected spheres consisted of $U(93)O_2(NO_3)_2$ and H_2O at various concentrations and with/without boron. ORNL-1, -2, and -3 have a radius of 34.595 cm, and ORNL-10 has a radius of 61.011 cm. The reported eigenvalues have an uncertainty of 0.25%.

The TRX experiments (51–52 of Table 1) are water-moderated lattices of slightly enriched (1.3%) uranium metal rods with diameters of 0.4915 cm in a triangular pitch. The pitches were set to 1.8060 and 2.1740 cm to define the TRX-1 and TRX-2 configurations, respectively. Both experiments were modeled using a cell-weighting step, which characterized the pin lattice, followed by a 1-D cylindrical model consisting of core radii of 26.2093 and 27.4419 cm, followed by a 20-cm-thick water reflector. In both cases an axial buckling height of 136.98 cm was assumed.

2.3 PCTR Experiments

This group of 11 experiments (35–45 of Table 1) were performed at the Physical Constants Test Reactor (PCTR)[14] and consisted of the measurement of k_∞ for three different enrichments near 1.0 wt %, with variable H/U values. The experiments are identified by their respective H/U values: 3.83, 6.23, 6.95, and 7.52, which have an enrichment of 1.006 wt %; 3.78, 5.84, and 7.14, which have enrichments of 1.071 wt %; and 3.73, 5.99, 6.90, and 7.52, which have enrichments of 1.157 wt %. The experimentally inferred values of k_∞ are given in Table 2, along with their uncertainties.

Table 2 PCTR central region experiments[a]

Case No.	^{235}U wt %	H/U	Exp. *k*
1	1.006	3.83	0.986
2	1.006	6.23	0.986
3	1.006	6.95	0.974
4	1.006	7.52	0.960
5	1.071	3.78	1.005
6	1.071	5.84	1.005
7	1.071	7.14	0.992
8	1.157	3.73	1.031
9	1.157	5.99	1.031
10	1.157	6.90	1.030
11	1.157	7.52	1.019

[a]Experimental uncertainty is ± 0.006 Δk (varies from 0.005 to 0.007).

2.4 HEUMET Systems

This group of nine experiments (21–29 of Table 1) include two separate measurement sets.[15] The first is a single experiment consisting of a water-reflected U(98) metal sphere with radii corresponding to 6.5537 cm for the core and 33.4717 cm for the reflector. The remaining set consists of eight experiments with a U(93.5) metal (Oralloy) core, along with variable thickness reflectors of natural uranium (Tuballoy) or nickel. The dimensions are given in Table 3 for each of these situations.

Table 3 Dimensions for Tuballoy- and nickel-reflected spheres[a]

Reflector thickness (in)	Region	Outer radius (cm)	Material
2.0	1	6.7820	Oralloy
	2	11.8620	Tuballoy
3.0	1	6.4423	Oralloy
	2	14.0623	Tuballoy
4.0	1	6.2851	Oralloy
	2	16.4451	Tuballoy
5.0	1	6.1535	Oralloy
	2	18.8535	Tuballoy
7.0	1	6.0740	Oralloy
	2	23.8540	Tuballoy
8.0	1	6.0509	Oralloy
	2	26.3709	Tuballoy
11.0	1	6.0276	Oralloy
	2	33.9676	Tuballoy
8.0	1	6.4627	Oralloy
	2	26.7827	Ni

[a]The experimental values of k_{eff} for all cases is 1.000, with uncertainties in the experiments of ±0.003 for reflector thicknesses of 5, 7, 8, and 11 in. and ±0.005 for all others.

2.5 Rocky Flats Experiments

These experiments[16, 17] consist of a series of measurements (59–66 in Table 1) corresponding to low-enrichment and low-moderation conditions. The fuel in all cases was $U(4.5)O_2$, which was packed into 1.6-mm-thick aluminum cans forming a 152-mm cube. Water was added to the oxide to achieve H/U ratios of 0.77 and 2.03. The experimental setup consisted of reflected 5 × 5 × 5 arrays of these cans typically driven by a high-enriched uranium driver to achieve criticality. The drivers were a high-enriched uranium metal sphere, and high- and low-concentration uranyl nitrate solution boxes.

Eight configurations were included in this work, four each for the H/U ratios of 0.77 and 2.03. The 1-D spherical models shown in Tables 4 and 5 were generated based on conservation of the actual experimental volumes.

Table 4 Spherical models for Rocky Flats H/U = 0.77 experiments

Configuration	Region	Outer radius (cm)	Material
RF H/U = 0.77 A	1	7.334	U metal
	2	9.454	Air
	3	49.627	Hom. $UO_2 + H_2O + Al$
	4	75.227	Plastic reflector
RF H/U = 0.77 B	1	11.958	High conc. solution
	2	14.769	Void
	3	15.015	Steel
	4	49.600	Hom. $UO_2 + H_2O + Al$
	5	75.200	Concrete reflector
RF H/U = 0.77 C	1	12.248	High conc. solution
	2	14.769	Void
	3	15.015	Steel
	4	49.656	Hom. $UO_2 + H_2O + Al$
	5	75.256	Plastic reflector
RF H/U = 0.77 D	1	13.041	Low conc. solution
	2	14.746	Void
	3	14.983	Steel
	4	49.650	Hom. $UO_2 + H_2O + Al$
	5	75.250	Plastic reflector

[a]The experimental values are 1.000, the uncertainties in the measured values of k_{eff} are not explicitly quoted, but are estimated to be ±0.001.

Table 5 Spherical models for Rocky Flats H/U = 2.03 experiments[a]

Configuration	Region	Outer radius (cm)	Material
RF H/U = 2.03 A	1	34.857	Hom. UO_2 + H_2O + Al + Poly (0.93 cm)
	2	60.457	Plastic reflector
RF H/U = 2.03 B	1	32.628	Hom. UO_2 + H_2O + Al + Poly (2.44 cm)
	2	58.228	Plastic reflector
RF H/U = 2.03 C	1	5.669	U metal
	2	9.454	Void
	3	45.919	Hom. UO_2 + H_2O + Al
	4	71.519	Plastic reflector
RF H/U = 2.03 D	1	2.340	Void
	2	5.670	U metal
	3	9.454	Void
	4	45.746	Hom. UO_2 + H_2O + Al
	5	71.346	Plastic reflector

[a]The experimental values are 1.000, the uncertainties in the measured values of k_{eff} are not explicitly quoted, but are estimated to be ±0.001.

2.6 Russian Critical Experiments

The Russian experiments included in this work (67–102 of Table 1) have been documented in the Benchmark Handbook[7] and separately described and analyzed in another phase of this work.[8] These experiments include HEU-SOL-THERM-029 (7 configurations), HEU-SOL-THERM-030 (7 configurations), HEU-SOL-THERM-031 (4 configurations), IEU-COMP-THERM-02 (6 configurations), LEU-COMP-THERM-32 (9 configurations), and LEU-SOL-THERM-005 (3 configurations). Each of these configurations was modeled in 1-D. The models and results from these 1-D studies are given in Ref. 8.

2.7 Other Systems

The first two systems (49–50 of Table 1) included in this group are the UH3-UR and UH3-NI critical assemblies.[18] These assemblies consist of approximate spheres of enriched-uranium hydride within a 20.32-cm thick natural uranium and nickel reflectors. The average empirical formula of the hydride composition is $U(93.15)H_{2.97}C_{1.11}O_{0.25}$. The benchmarks are modeled as a sphere within a 20.32 cm natural uranium reflector (UH3-UR) and a 20.32 cm nickel reflector (UH3-NI). The UH3-UR core has a radius of 7.7902 cm, and the UH3-NI has a core radius of 7.7978 cm. The reported value of k_{eff} is 1.000 with no uncertainties quoted.

The HISS benchmarks are measurements of k_{eff} and are based on central region experiments.[19] The single experiment considered in this work (20 of Table 1) is the homogeneous uranium graphite (HUG) measurement. The HISS(HUG) contains HEU plus graphite with a graphite/U-235 ratio of 302, and a boron/U-235 ratio of 1.16. The measured value of k_{eff} for this system is 1.000 ± 0.004.

The ORNL L-7 to L-11 experiments[20] are a family of criticals (53–57 of Table 1) that consist of reflected and unreflected spheres of uranyl fluoride in water. Details of the models for each of these systems are given in Table 6. The vessel wall is made of aluminum. The measured k_{eff} values for each experiment are also given in the table. No uncertainty on these values is quoted. A 20-cm-thick region of water at room temperature was assumed for the reflector.

The SHEBA experiment[15] is an unreflected cylinder of $U(5)O_2F_2 + H_2O$. The sensitivity calculations for this experiment were performed with a 2-dimensional model and the SEN2 code.

Table 6 Benchmark descriptions for ORNL L-8 to L-11 experiments

Assembly	Measured k_{eff}	Inner radius (cm)	Vessel wall thickness (cm)	H/X	Water reflector
L-7	1.0000	11.5176	0.16	76.1	Yes
L-10	1.0000	11.8442	0.16	126.5	Yes
L-8	1.0004	27.9132	0.20	1112	No
L-11	0.9999	27.9132	0.20	1276	Yes
L-9	1.0000	34.6327	0.32	1393	No

2.8 Tabulation of Calculated-versus-Experimental Results and Uncertainties

The calculated values of k_{eff} and associated sensitivity profiles for the set of 102 benchmark experiments described above were evaluated using the sensitivity analysis modules SEN1 (1-D models) and SEN2 (2-D models).[21] The cross-section library used in the analyses was the SCALE 44-group library[22] which is derived from a 238-group library processed from ENDF/B-V.[23] The necessary cross-section covariances were processed from ENDF/B-V into the 44-group structure. In most cases, the value of k_{eff} was based on the 1-D models also described above. In certain cases, like the Rocky Flats experiments, the values of k_{eff} are based on 3-D Monte Carlo (KENO V.a) models, although the sensitivity results are based on 1-D models. This "substitution" is necessary because the 1-D models for these cases contain significant model bias, which should be accounted for in order for the GLLSM techniques to be valid.

In Table 7, the calculated k_{eff} values of each of the 102 benchmark experiments are presented, along with their uncertainty due to cross-section uncertainties. The uncertainties in the system specification are included in the measurement uncertainties by convention. The uncertainties in the calculated k_{eff} values were estimated using the SEN1 or SEN2 modules, which incorporates the S/U methodology presented in Vol. 1 of this report. The measured k_{eff} values are also presented, along with their estimated uncertainties. The uncertainties in the measured values are incomplete, since a great deal of work is needed in most cases to quantify these values.

Table 7 Measured-versus-calculated k_{eff} values for 102 critical benchmarks

System No.	Calculated k_{eff} value	Uncertainty in calculated k_{eff}, % std. dev.	Measured k_{eff} value	Uncertainty in measured k_{eff}, % std. dev.	(Measured/ calculated) - 1, %
1 U(2)F4 - 195	1.0065	1.6	1.000	0.5	-0.65
2 U(2)F4 - 294	1.0079	1.4	1.000	0.4	-0.79
3 U(2)F4 - 406	1.0049	1.3	1.000	0.5	-0.49
4 U(2)F4 - 496	1.0029	1.2	1.000	0.4	-0.29
5 U(2)F4 - 614	1.0020	1.2	1.000	0.4	-0.20
6 U(2)F4 - 972	0.9954	1.1	1.000	0.5	0.46
7 U(3)F4 - 133	1.0219	1.6	1.000	0.5	-2.15
8 U(3)F4 - 277	1.0193	1.3	1.000	0.5	-1.90
9 U(5)3O8 - 147	0.9964	1.3	1.000	0.4	0.36
10 U(5)3O8 - 245	0.9839	1.1	1.000	0.4	1.63
11 U(5)3O8 - 320	1.0077	1.1	1.000	0.4	-0.76
12 U(5)3O8 - 396	1.0021	1.0	1.000	0.3	-0.21
13 U(5)3O8 - 503	1.0013	1.0	1.000	0.3	-0.13
14 U(5)3O8 - 757	1.0038	0.9	1.000	0.3	-0.38
15 Godiva	1.0041	1.6	1.000	0.1	-0.41
16 Bapl-1	1.0017	1.2	1.000	NR *	-0.17
17 Bapl-2	1.0016	1.1	1.000	NR	-0.16
18 Bapl-3	1.0023	1.0	1.000	NR	-0.23
19 Big-10	1.0173	1.7	1.000	0.3	-1.70
20 HISS (HUG)	1.0119	2.1	1.000	0.4	-1.18
21 U(98) H2O refl.	0.9986	1.4	1.000	0.5	0.14
22 HEUMET A	0.9881	1.6	1.000	0.5	1.21
23 HEUMET B	0.9865	1.6	1.000	0.5	1.37
24 HEUMET C	0.9911	1.6	1.000	0.5	0.90
25 HEUMET D	0.9897	1.6	1.000	0.3	1.04
26 HEUMET E	0.9956	1.6	1.000	0.3	0.45
27 HEUMET F	0.9966	1.6	1.000	0.3	0.34
28 HEUMET G	0.9988	1.6	1.000	0.3	0.12
29 HEUMET H	1.0048	1.8	1.000	0.5	-0.48
30 ORNL-1	0.9990	0.8	1.000	0.3	0.10
31 ORNL-2	0.9987	0.8	1.000	0.3	0.13
32 ORNL-3	0.9957	0.8	1.000	0.3	0.43
33 ORNL-4	0.9972	0.8	1.000	0.3	0.29
34 ORNL-10	0.9991	0.9	1.000	0.3	0.09

Table 7 (continued)

System No.	Calculated k_{eff} value	Uncertainty in calculated k_{eff}, % std. dev.	Measured k_{eff} value	Uncertainty in measured k_{eff}, % std. dev.	(Measured/ calculated) - 1, %
35 PCTR 3.73	1.0342	1.5	1.031	0.6	-0.31
36 PCTR 3.78	1.0099	1.5	1.005	0.6	-0.49
37 PCTR 3.83	0.9897	1.5	0.986	0.6	-0.37
38 PCTR 5.84	1.0097	1.3	1.005	0.6	-0.47
39 PCTR 5.99	1.0370	1.3	1.031	0.6	-0.58
40 PCTR 6.23	0.9829	1.3	0.986	0.6	0.32
41 PCTR 6.90	1.0293	1.3	1.030	0.6	0.07
42 PCTR 6.95	0.9750	1.3	0.974	0.6	-0.10
43 PCTR 7.14	0.9971	1.3	0.992	0.6	-0.51
44 PCTR 7.52	0.9678	1.2	0.960	0.6	-0.80
45 PCTR 7.52a	1.0225	1.2	1.019	0.6	-0.34
46 ZPR 3/11	1.0201	1.7	1.000	0.3	-1.97
47 ZPR 3/12	1.0138	1.6	1.000	0.2	-1.36
48 ZPR 6/6a	1.0247	1.9	1.000	0.1	-2.41
49 UH3 NI	1.0108	1.9	1.000	NR	-1.07
50 UH3 UR	1.0072	1.6	1.000	NR	-0.71
51 TRX-1	0.9947	1.1	1.000	NR	0.53
52 TRX-2	0.9975	0.9	1.000	NR	0.25
53 ORNL L7	1.0053	0.9	1.000	NR	-0.53
54 ORNL L8	1.0063	0.8	1.0004	NR	-0.63
55 ORNL L9	1.0034	0.8	1.000	NR	-0.34
56 ORNL L10	1.0029	0.8	1.000	NR	-0.29
57 ORNL L11	1.0016	0.8	0.9999	NR	-0.16
58 SHEBA	1.0089	1.0	1.000	NR	-0.88
59 RF 0.77 A	1.0037	1.3	1.000	0.1	-0.37
60 RF 0.77 B	1.0116	1.1	1.000	0.1	-1.15
61 RF 0.77 C	1.0061	0.9	1.000	0.1	-0.61
62 RF 0.77 D	1.0107	1.2	1.000	0.1	-1.06
63 RF 2.03 A	1.0062	1.3	1.000	0.1	-0.62
64 RF 2.03 B	1.0105	1.0	1.000	0.1	-1.04
65 RF 2.03 C	1.0065	1.5	1.000	0.1	-0.65
66 RF 2.03 D	1.0001	1.5	1.000	0.1	-0.01
67 HST29-1	1.0032	1.1	1.000	0.7	-0.32
68 HST29-2	1.0062	1.1	1.000	0.6	-0.62
69 HST29-3	1.0002	1.1	1.000	0.7	-0.02

Table 7 (continued)

System No.	Calculated k_{eff} value	Uncertainty in calculated k_{eff}, % std. dev.	Measured k_{eff} value	Uncertainty in measured k_{eff}, % std. dev.	(Measured/ calculated) - 1, %
70 HST29-4	0.9964	1.1	1.000	0.7	0.36
71 HST29-5	1.0015	1.1	1.000	0.7	-0.15
72 HST29-6	1.0050	1.1	1.000	0.7	-0.50
73 HST29-7	1.0031	1.1	1.000	0.6	-0.31
74 HST30-1	1.0002	1.0	1.000	0.4	-0.02
75 HST30-2	1.0006	1.0	1.000	0.3	-0.06
76 HST30-3	0.9995	1.0	1.000	0.3	0.05
77 HST30-4	1.0046	1.1	1.000	0.6	-0.46
78 HST30-5	1.0006	1.1	1.000	0.6	-0.06
79 HST30-6	1.0024	1.1	1.000	0.6	-0.24
80 HST30-7	1.0007	1.3	1.000	0.6	-0.07
81 HST31-1	1.0012	1.1	1.000	0.5	-0.12
82 HST31-2	1.0035	1.1	1.000	0.6	-0.35
83 HST31-3	1.0027	1.1	1.000	0.6	-0.27
84 HST31-4	1.0000	1.1	1.000	0.7	0.00
85 ICT02-1	0.9944	1.0	1.000	0.4	0.56
86 ICT02-2	0.9927	1.0	1.000	0.4	0.74
87 ICT02-3	0.9997	1.0	1.000	0.4	0.03
88 ICT02-4	0.9953	1.0	1.000	0.4	0.47
89 ICT02-5	0.9927	1.0	1.000	0.4	0.74
90 ICT02-6	0.9915	1.0	1.000	0.4	0.86
91 LCT32-1	0.9977	1.2	1.000	0.4	0.23
92 LCT32-2	0.9912	1.3	1.000	0.4	0.89
93 LCT32-3	0.9881	1.3	1.000	0.4	1.20
94 LCT32-4	1.0095	1.0	1.000	0.4	-0.94
95 LCT32-5	0.9977	1.0	1.000	0.3	0.23
96 LCT32-6	0.9982	1.0	1.000	0.3	0.18
97 LCT32-7	1.0079	1.0	1.000	0.5	-0.78
98 LCT32-8	1.0020	1.0	1.000	0.4	-0.20
99 LCT32-9	1.0026	1.0	1.000	0.4	-0.26
100 LST05-1	0.9988	1.1	1.000	0.4	0.12
101 LST05-2	0.9989	1.1	1.000	0.5	0.11
102 LST05-3	0.9989	1.1	1.000	0.6	0.11

*None reported (NR)

A complete analysis of the measurement uncertainties was carried out on the first 14 experiments. The details of this analysis are described in Section 4 to serve as guidance on the generation of similar results for all systems included in a GLLSM analysis.

For the purposes of this work, a range of measurement uncertainties corresponding to 0.1 to 0.4% was assumed. Various scenarios were assumed to determine the sensitivity of the final results to the explicit values assumed for the measurement uncertainties. This procedure should be useful in establishing a standard approach toward the estimation of measurement uncertainties.

3 USE OF METHODOLOGY FOR GREATER THAN 5-WT % ENRICHED URANIUM APPLICATIONS

The GLLSM methodology, as described in Volume 1 of this document,[6] is quite complex and may be quite daunting to the criticality safety practitioner. For this reason, this section is designed to proceed through a criticality validation exercise using standard techniques, S/U techniques, and GLLSM techniques as demonstration exercises. Each of these techniques will use the same benchmark database which consists of the 102 experiments described in the previous section. These experiments are not specifically "tailored" for the greater than 5 wt % applications; they represent a generic set which could be used for a number of different applications using these new validation techniques. The S/U and GLLSM approaches have several options, which will be examined; conclusions will be drawn from the various approaches.

3.1 Description of $U(11)O_2$ Systems

The illustrative application for which validation is sought is a series of $U(11)O_2$ systems with H/X values of 0, 3, 5, 10, 20, 40, 80, 200, 300, 400, 500, 600, 800, and 1000. These $U(11)O_2$ systems are "artificial" critical bare spheres generated for calculational comparison purposes. The object of this demonstration problem is the validation of the underlying cross sections and criticality code for these 14 systems.

The dimensions for the $U(11)O_2$ systems were generated via a critical radius search calculation using the SCALE/XSDRNPM module. The critical radii corresponding to the 14 unreflected systems for H/X of 0 to 1000 were 50.55, 40.00, 36.85, 31.77, 26.48, 22.34, 19.87, 18.99, 19.53, 20.39, 21.42, 22.51, 25.41, and 29.17 cm.

3.2 Sensitivity and Uncertainty Analyses of the $U(11)O_2$ Systems

These 14 systems were analyzed with the SEN1 sensitivity module, which generates detailed sensitivity information, as well as the uncertainty in the system k_{eff} value due to cross-section uncertainties obtained from the Evaluated Nuclear Data Files (ENDF/B). The same cross-section library (SCALE 44-group) and associated covariances used in the analysis of the critical experiments were used for the analysis of these 14 applications. Using this sensitivity and uncertainty information, the uncertainty in the calculated value of k_{eff} for each system can be generated. Also, the covariance of any two systems can easily be determined. To illustrate, Table 8 provides the uncertainty matrix for the 14 $U(11)O_2$ systems. This matrix gives the system uncertainty for the calculated k_{eff} on the diagonal and the correlation coefficient on the off-diagonal element. These off-diagonal elements are the c_k parameters, and can be used for defining similar systems. Such a matrix can also be generated for the entire set of benchmark experiments plus applications. In this case, an 116 × 116 matrix was generated, corresponding to the 102 criticals and 14 applications. For this study, only a 14 × 102 matrix was necessary (i.e., each row corresponding to each of the 14 applications and 102 columns corresponding to each of the benchmarks). Shown in Figures 1–4 are rows of the full matrix corresponding to the $U(11)O_2$ systems for H/X values of 0, 3, 40 and 500. The values plotted correspond to the c_k coefficients for all 102 systems. (Note that labels are only given to every third system. The system order is the same as shown in Tables 1 and 7.) These plots allow, at a glance, the determination of the number of systems in the benchmark dataset that are similar to the particular application. From Figure 1, it is noted that 4 systems have c_k values at or greater than 0.9 compared to the H/X = 0 system. These values indicate that, based on the conclusions from Volume 1 where five systems with c_k of 0.9 or higher are suggested to ensure validation, the $U(11)O_2$ system with an H/X value of 0 is marginally covered by this benchmark set. However, it is clear from Figure 2 that the $U(11)O_2$ system with an H/X of 3 is *not* adequately covered by this

benchmark set. The remaining two graphs, shown in Figures 3–4, indicate that the $U(11)O_2$ systems with H/X values of 40 and 500 are adequately covered by this benchmark series.

Table 8 Correlation coefficients[a] for the $U(11)O_2$ systems

Critical system	11%-0	11%-3	11%-5	11%-10	11%-20	11%-40	11%-80	11%-200	11%-300	11%-400	11%-500	11%-600	11%-800	11%-1000
11% H/X = 0	**0.0191**													
11% H/X = 3	0.8328	**0.0185**												
11% H/X = 5	0.7379	0.9818	**0.0188**											
11% H/X = 10	0.6011	0.9205	0.9725	**0.0188**										
11% H/X = 20	0.4887	0.8409	0.9161	0.9784	**0.0176**									
11% H/X = 40	0.4067	0.7562	0.8403	0.9253	0.9763	**0.0151**								
11% H/X = 80	0.3428	0.6585	0.7392	0.8327	0.9094	0.9698	**0.0128**							
11% H/X = 200	0.2800	0.5240	0.5888	0.6760	0.7696	0.8705	0.9526	**0.0106**						
11% H/X = 300	0.2633	0.4751	0.5315	0.6115	0.7058	0.8157	0.9148	0.9832	**0.0099**					
11% H/X = 400	0.2557	0.4452	0.4953	0.5687	0.6604	0.7727	0.8798	0.9668	0.9846	**0.0095**				
11% H/X = 500	0.2517	0.4329	0.4688	0.5359	0.6235	0.7349	0.8453	0.9448	0.9717	0.9845	**0.0091**			
11% H/X = 600	0.2490	0.4076	0.4482	0.5097	0.5927	0.7014	0.8123	0.9200	0.9543	0.9742	0.9847	**0.0089**		
11% H/X = 800	0.2432	0.3755	0.4076	0.4567	0.5278	0.6265	0.7331	0.8514	0.8991	0.9330	0.9576	0.9734	**0.0087**	
11% H/X = 1000	0.2353	0.3452	0.3697	0.4071	0.4652	0.5509	0.6484	0.7702	0.8277	0.8731	0.9097	0.9367	0.9752	**0.0087**

[a]Note the diagonal element contains the fractional standard deviation instead of the correlation coefficient.

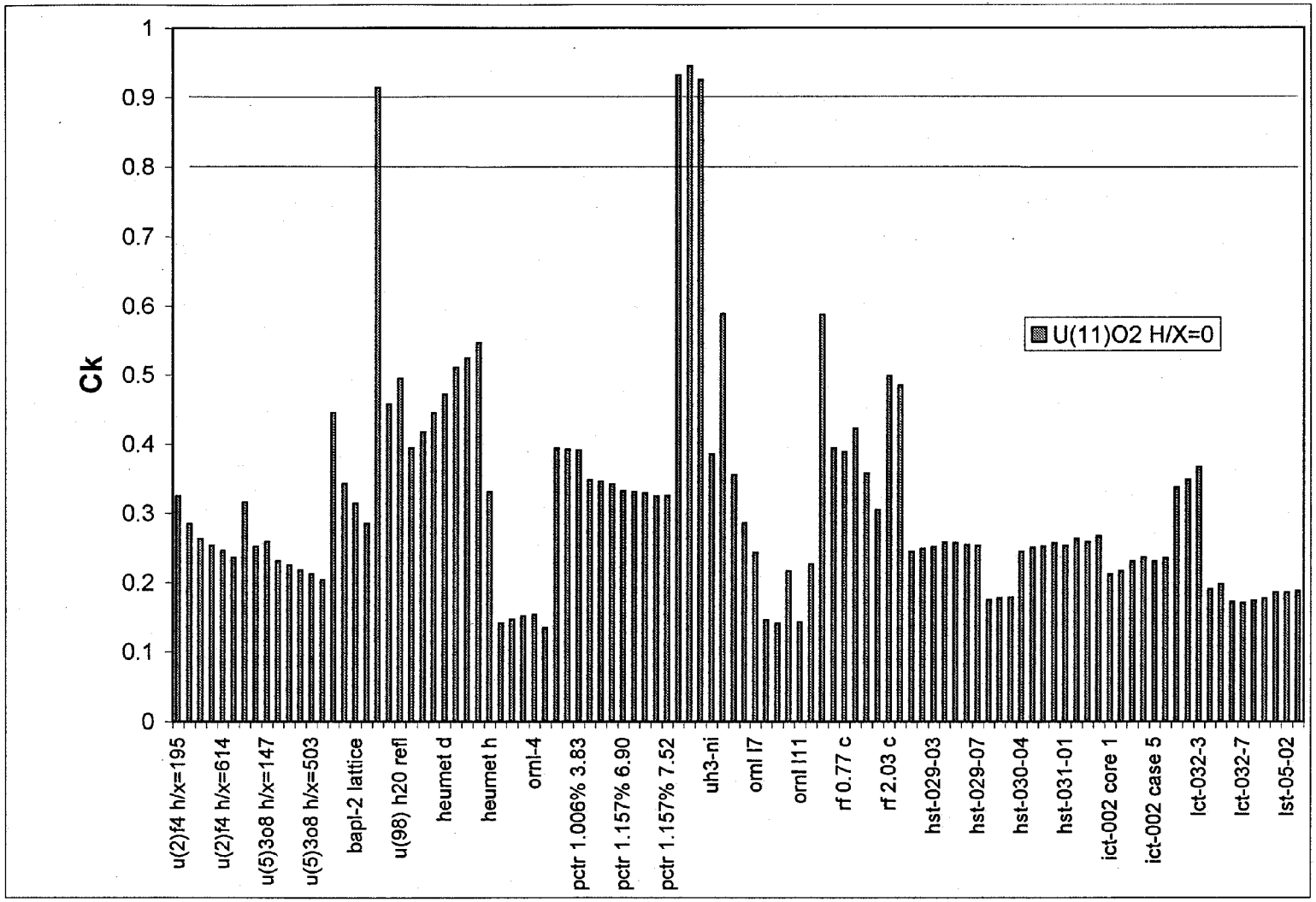

Figure 1 Correlation coefficients, c_k, for $U(11)O_2$, H/X = 0 system with 102 benchmark experiments

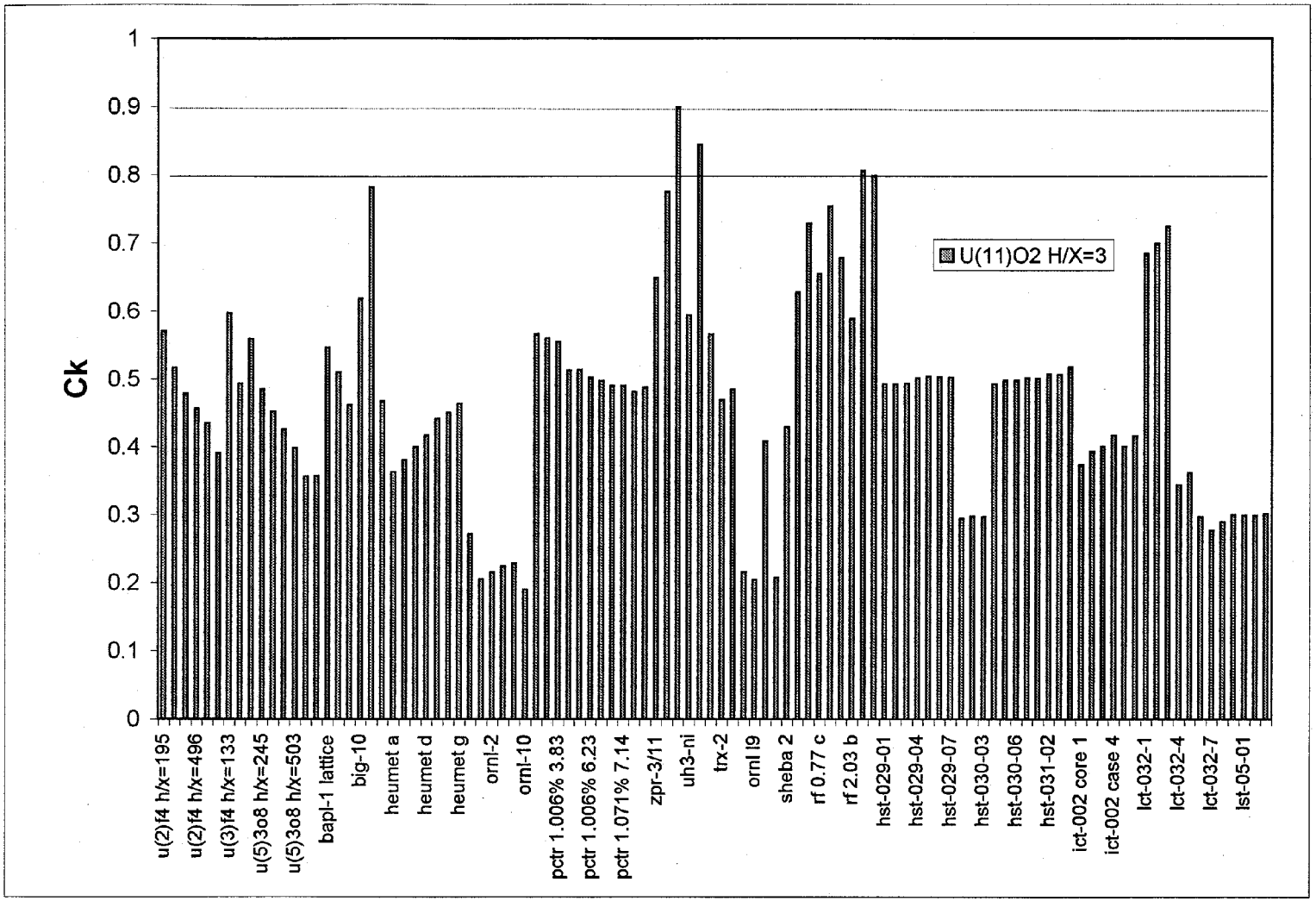

Figure 2 Correlation coefficients, c_k, for $U(11)O_2$, H/X = 3 system with 102 benchmark experiments

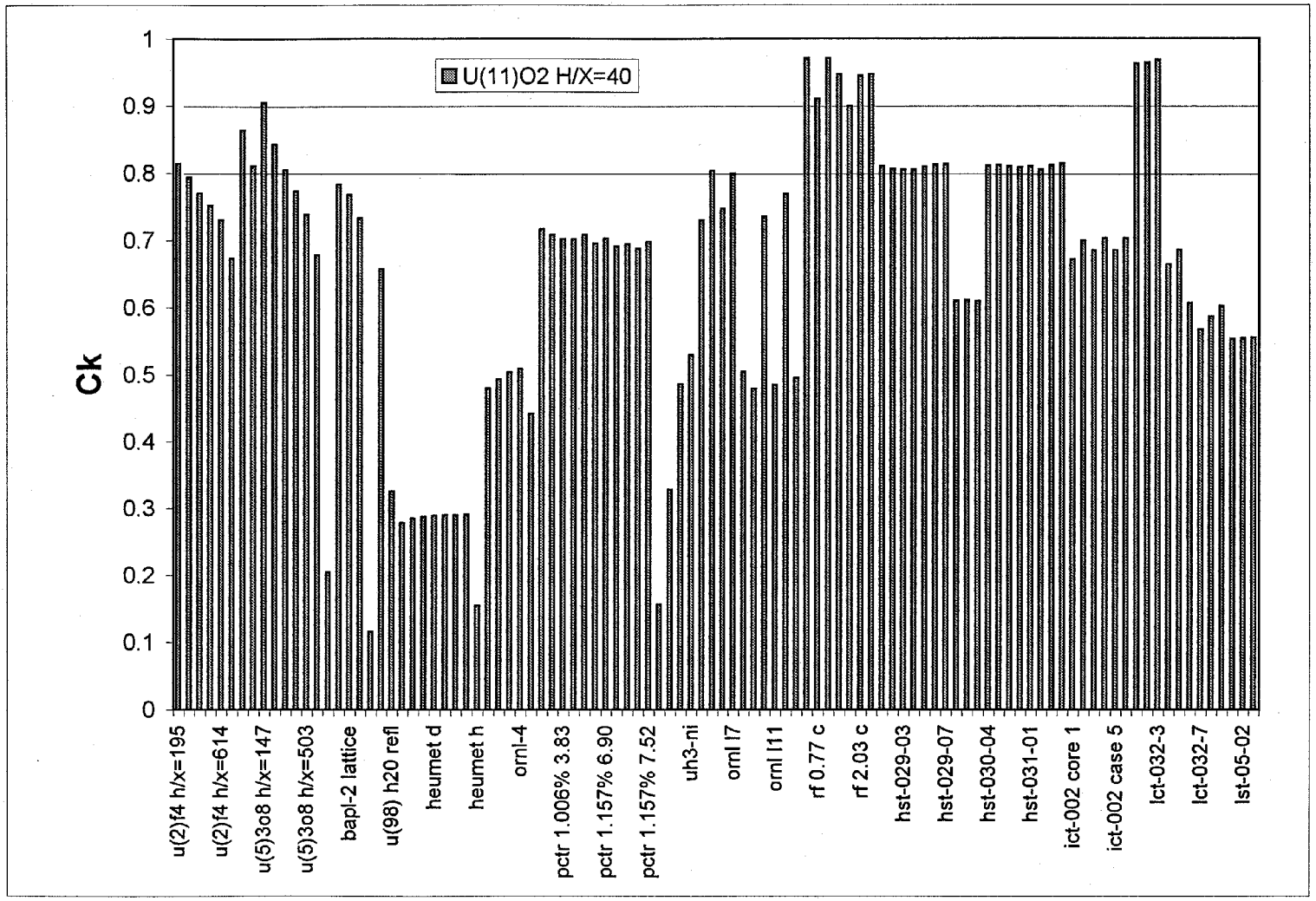

Figure 3 Correlation coefficients, c_k, for $U(11)O_2$, H/X = 40 system with 102 benchmark experiments

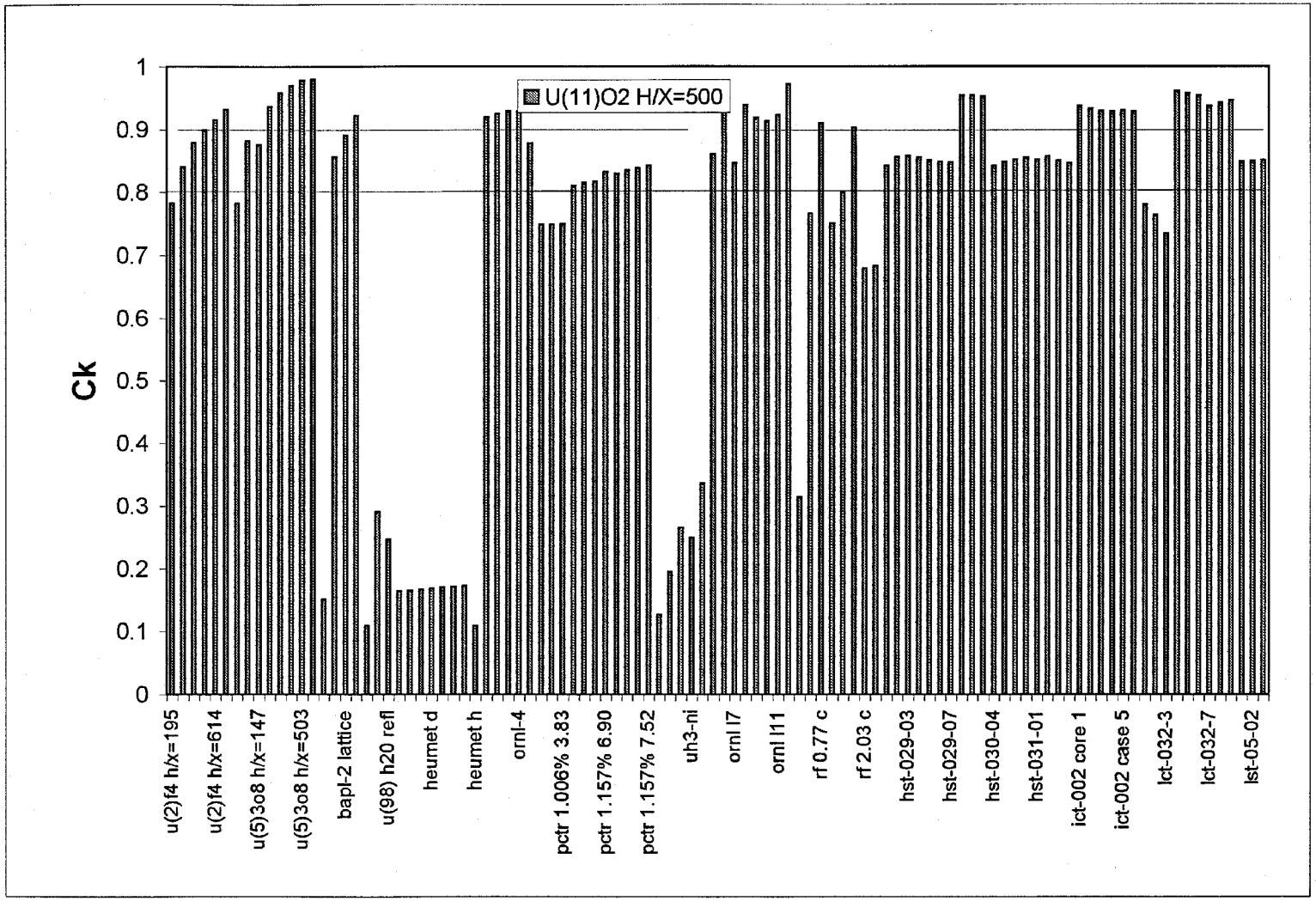

Figure 4 Correlation coefficients, c_k, for $U(11)O_2$, H/X = 500 system with 102 benchmark experiments

Similarly, a matrix of values corresponding to the D_c, D_n, and D_s values previously defined can also be generated based only on the sensitivity coefficients generated using the SEN1 module. In Figures 5–8, the sum of the D_c, D_n, and D_s values are plotted for the $U(11)O_2$ systems with H/X = 0, 3, 40, 500, respectively, to each of the 102 benchmark systems. Using this technique, the criterion for similar systems is that the sum of the D values should be less than about 1.2 (3 times the 0.4 criterion). In Figure 5, similarity is indicated for the $U(11)O_2$ H/X = 0 system and the same four systems previously determined to be similar. Figure 6 predicts similarity between the $U(11)O_2$ H/X = 3 system and only one other system. In Figures 7 and 8, the systems with H/X values 40 and 500 indicate about 10 and 40 systems, respectively, meet the less than 1.2 criterion. Hence, conclusions relative to system similarity based on these D coefficients agree with those of the preceding analysis using the c_k values.

3.3 Traditional Trending Analysis

In order to clearly show the relationship between the GLLSM techniques and the more traditional techniques for criticality safety validation, a traditional trending analysis using the same 102 benchmark experiments is presented. In Figure 9, k_{eff} is trended versus the energy of average lethargy causing fission (EALF). The prediction from this analysis would be a nearly constant positive bias of about 0.3%. Results shown in Figure 10 correspond to a similar parameter, energy of average lethargy causing capture (EALC). These results predict essentially the same biases as the EALF parameter and will not be further discussed.

Trend plots are also shown in Figures 11 and 12 for H/X and enrichment parameters. The H/X trend plot shows a slight trend, with the predicted Δk bias near zero for high H/X values and about +0.005 for low H/X values. The trend with enrichment is similar, but not enough data are present for the intermediate enrichments to confirm the trend.

Note that the largest variations (±2%) about the trend lines are seen for fast systems (i.e., the upper portion of the EALF, EALC trend plots and the lower portion of the H/X trend plot). Upon examination, it was observed for H/X = 0 systems that the predicted k_{eff} values less than unity were from the HEUMET set of criticals, while the systems with predicted eigenvalues greater than unity were from the Big-10 and ZPR sets. The combined effects of the high-versus-low enrichments and the processing of the SCALE 44-group library (collapsed using a thermal reactor spectrum) are believed to be responsible for this variation.

As a result of the trending analysis, a prediction of the Δk bias and its uncertainty can be obtained for each of the $U(11)O_2$ systems. Predictions using the USLSTATS procedure (Ref. 5) for systems with H/X values of 0, 3, 40, and 500 are given in Table 9.

Table 9 Predicted Δk bias and its standard deviation[a] based on traditional trending procedure

Trending Parameters	H/X = 0 System		H/X = 3 System		H/X = 40 System		H/X = 500 System	
	% bias	% std. dev. of biased k_{eff}	% bias	% std. dev. of biased k_{eff}	% bias	% std. dev. of biased k_{eff}	% bias	% std. dev. of biased k_{eff}
EALF	0.17	0.70	0.26	0.70	0.26	0.70	0.26	0.70
H/X	0.32	0.71	0.32	0.71	0.31	0.71	0.17	0.71

[a]Standard deviations correspond to the "pooled standard deviation" as specified in Ref. 5.

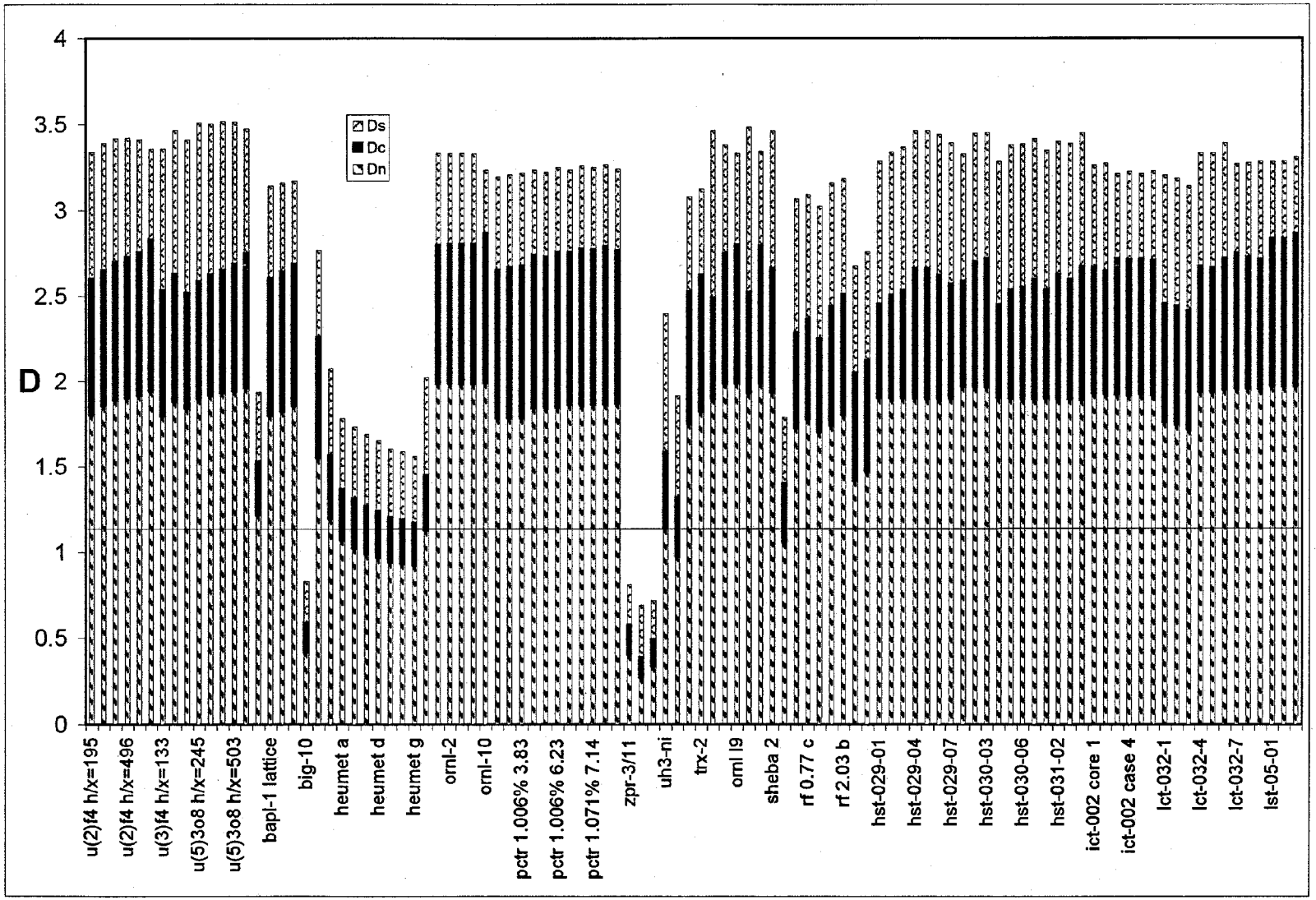

Figure 5 D coefficients for $U(11)O_2$, H/X = 0 system with 102 benchmark experiments

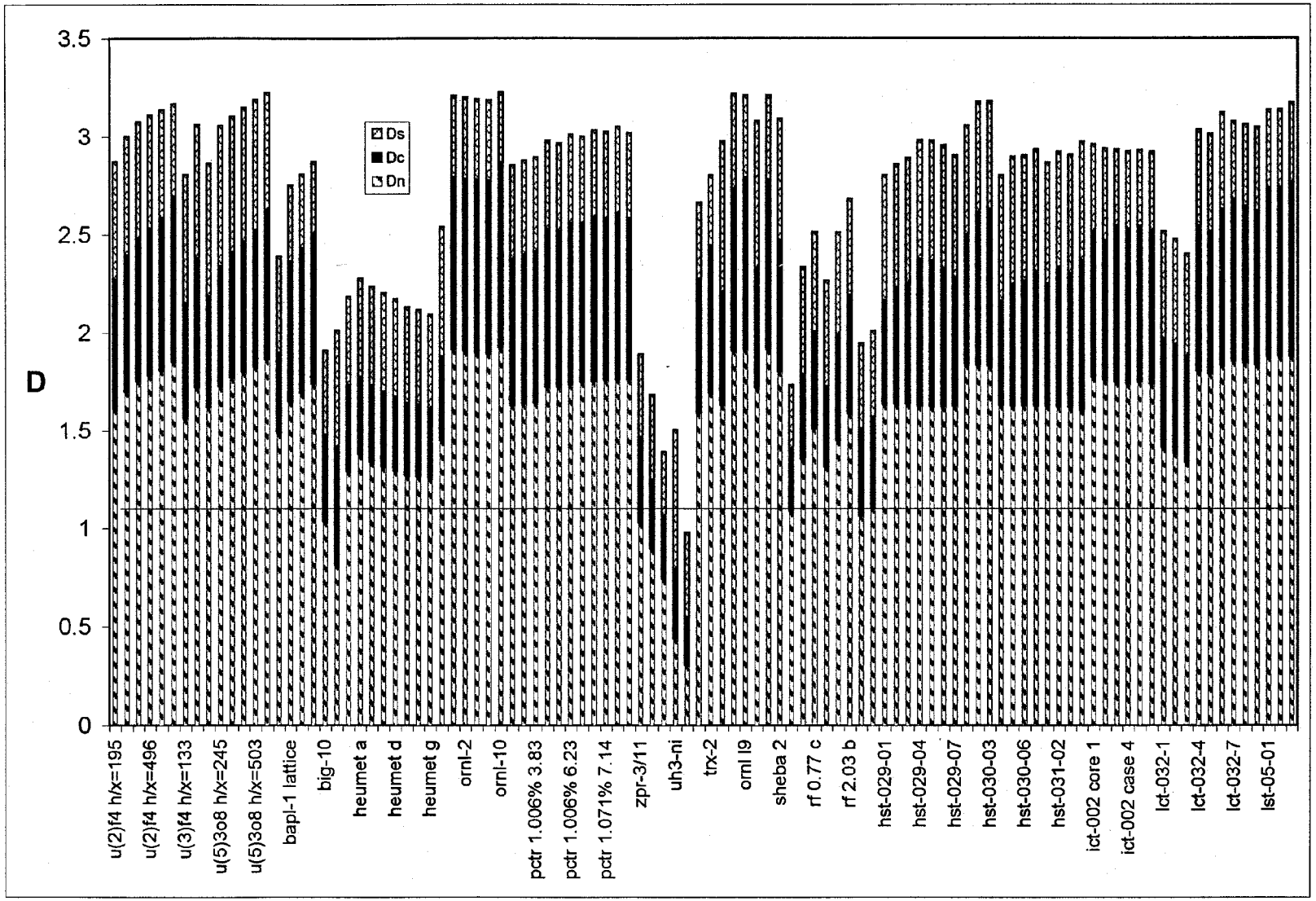

Figure 6 D coefficients for $U(11)O_2$, H/X = 3 system with 102 benchmark experiments

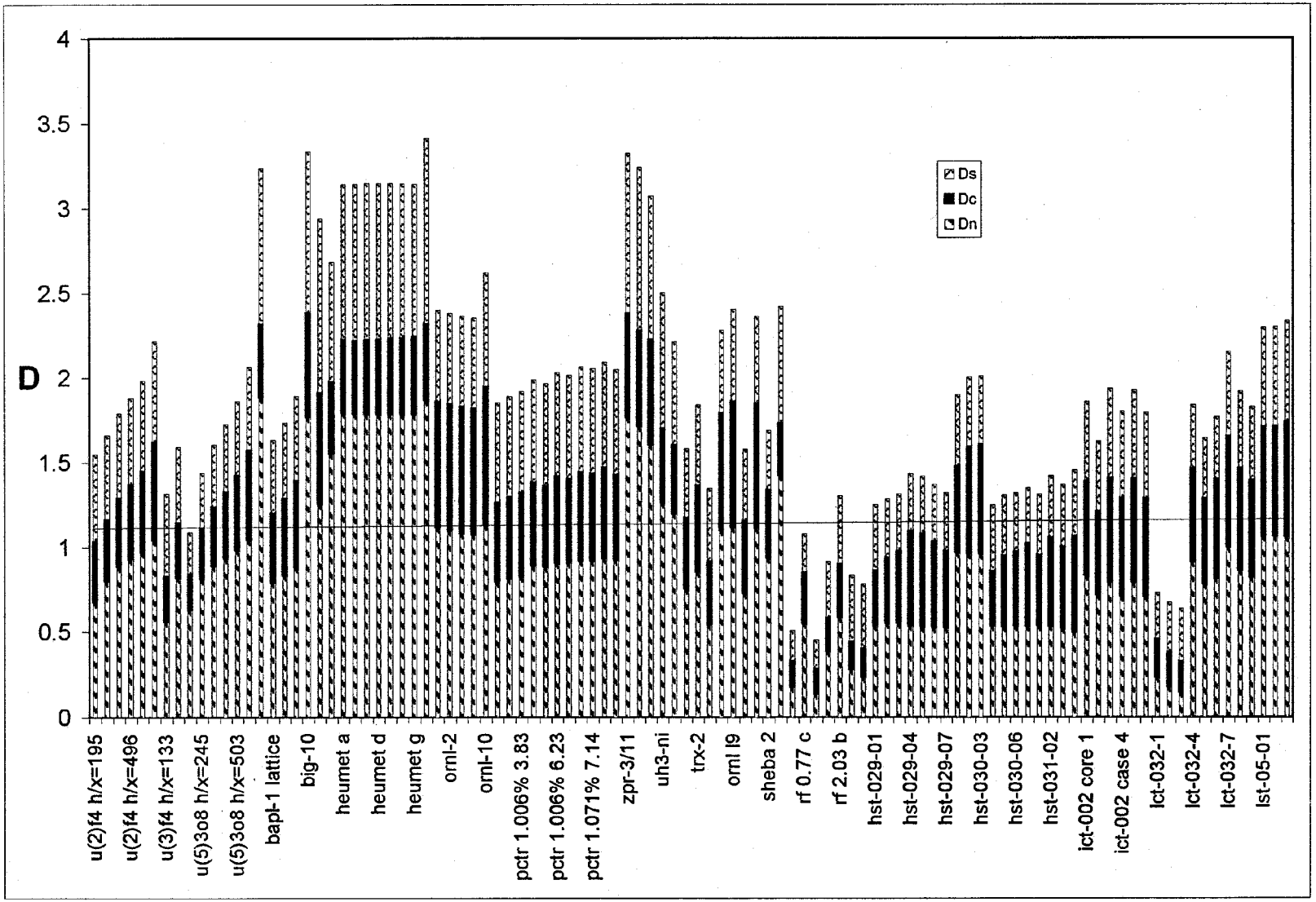

Figure 7 D coefficients for $U(11)O_2$, H/X = 40 systems with 102 benchmark experiments

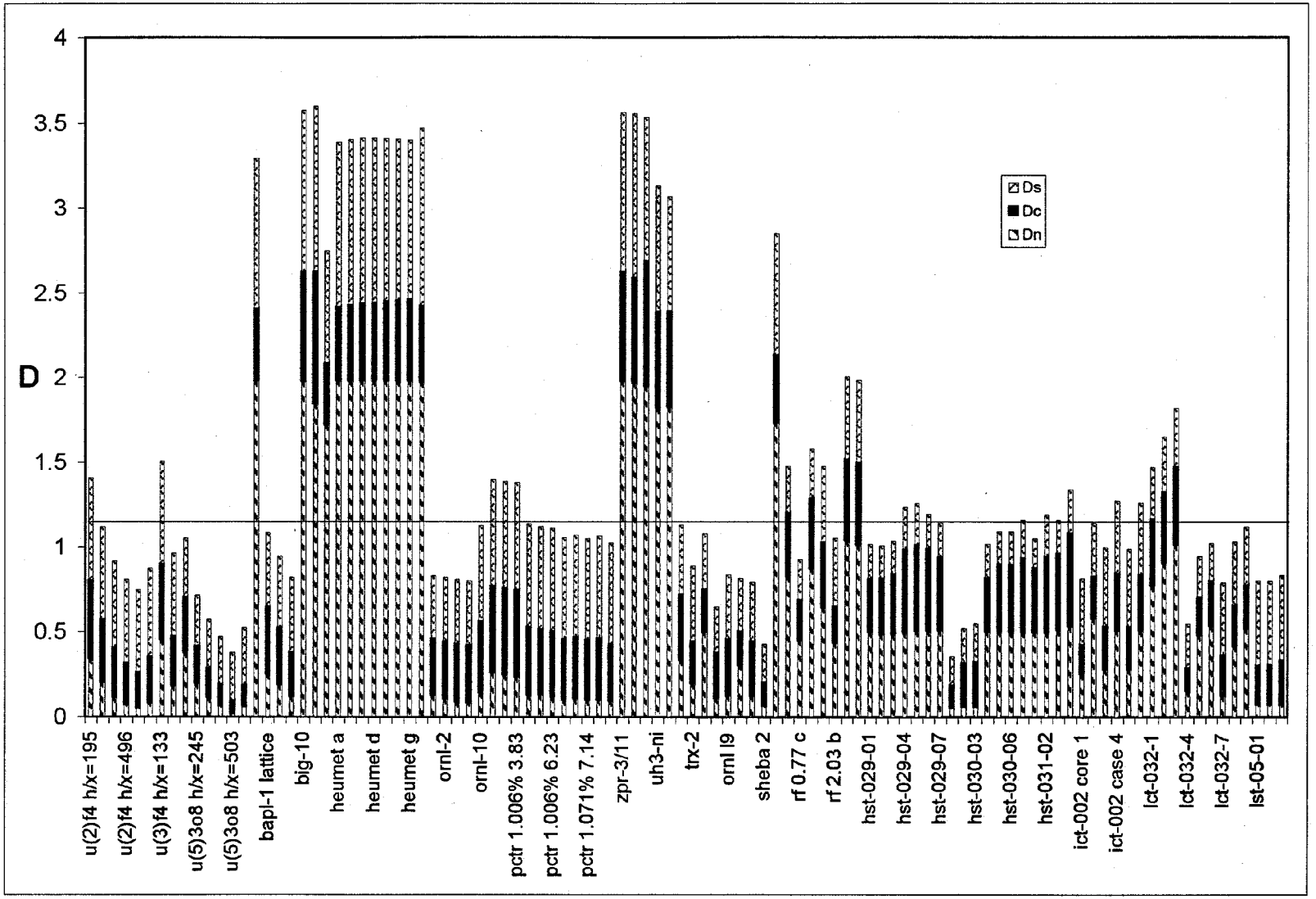

Figure 8 D coefficients for $U(11)O_2$, H/X = 500 system with 102 benchmark experiments

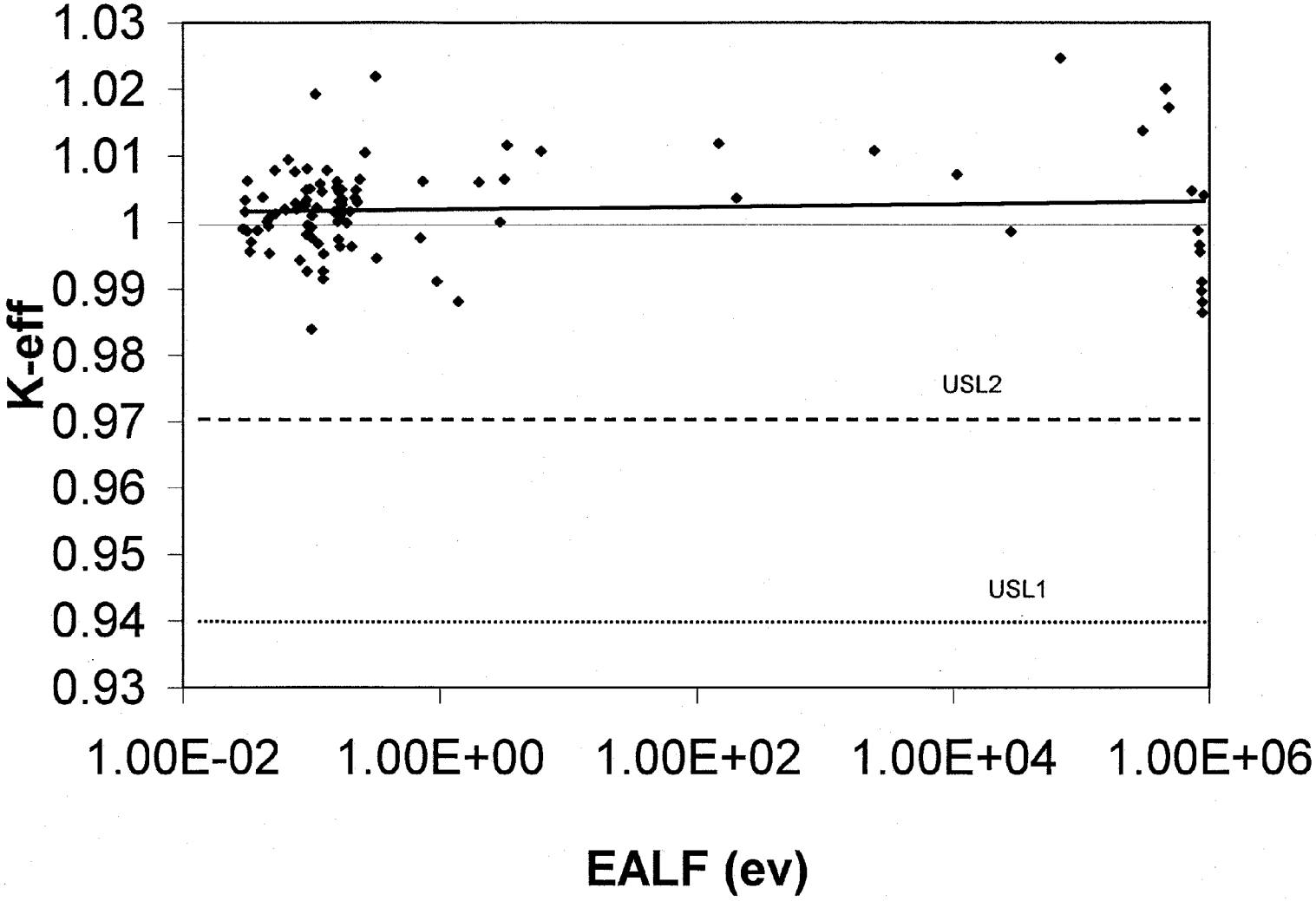

Figure 9 Trend plot for k_{eff} versus energy of average lethargy causing fission (EALF)

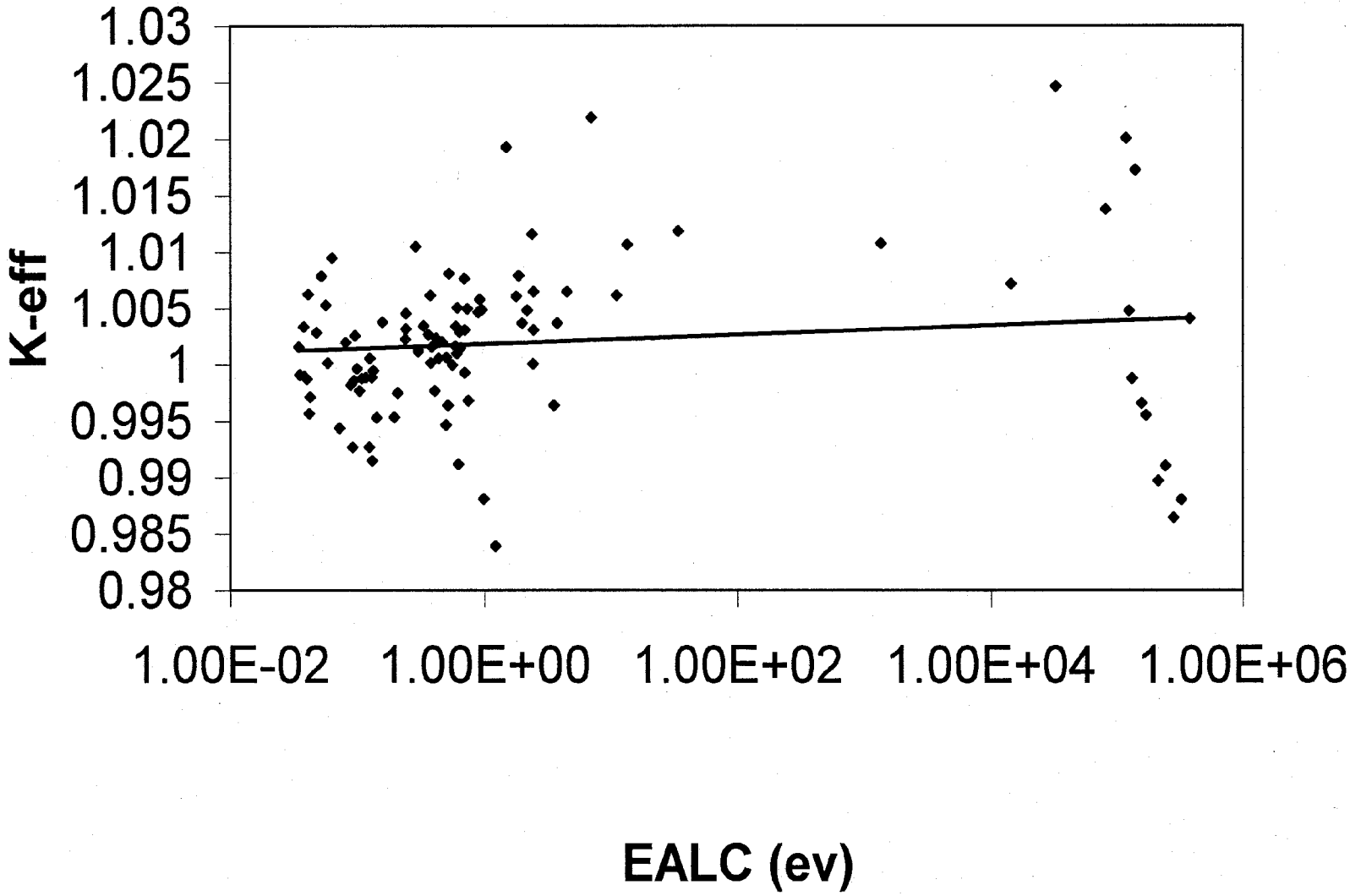

Figure 10 Trend plot for k_{eff} versus energy of average lethargy causing capture (EALC)

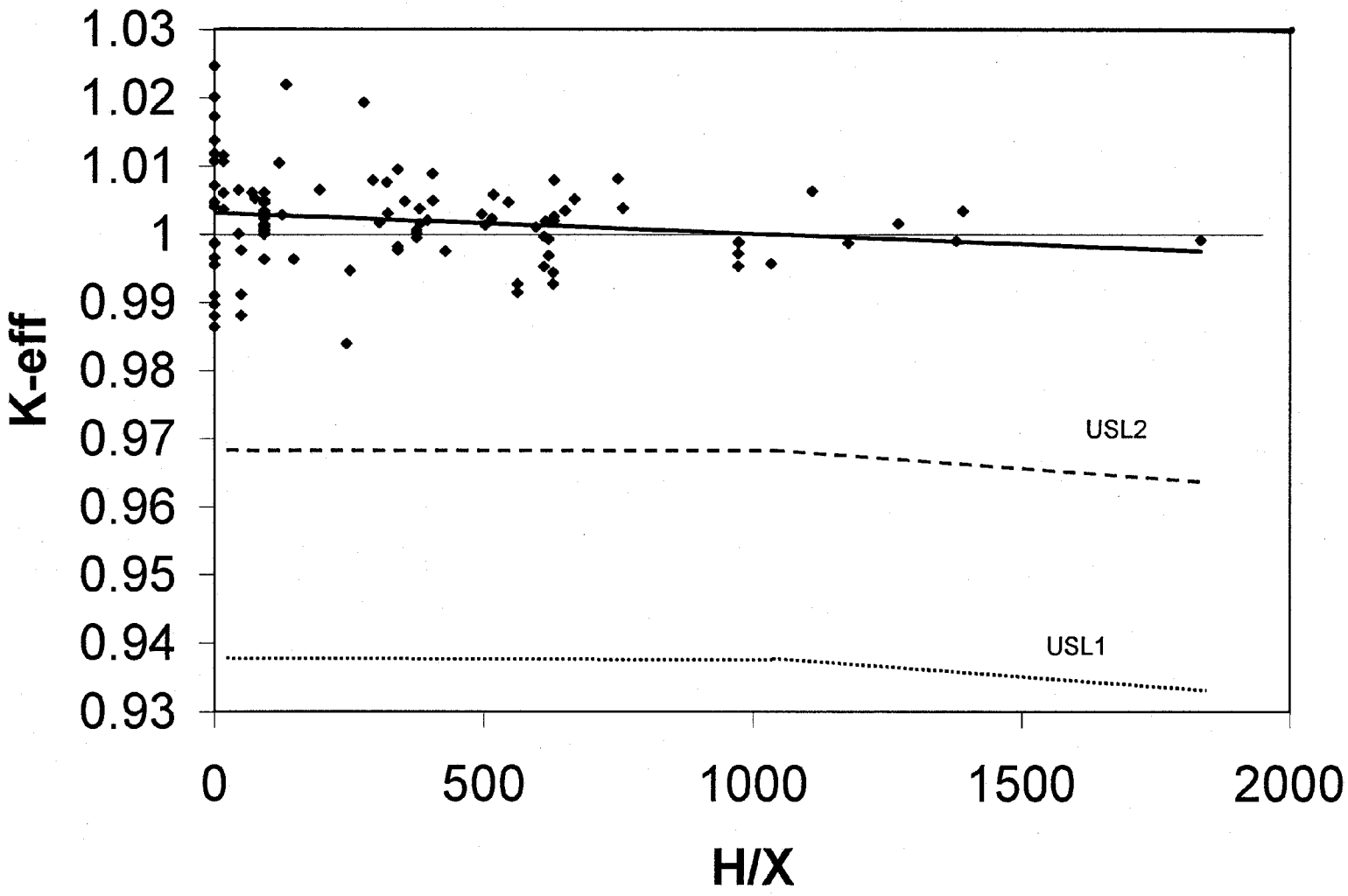

Figure 11 Trend plot for k_{eff} versus hydrogen-to-^{235}U ratio (H/X)

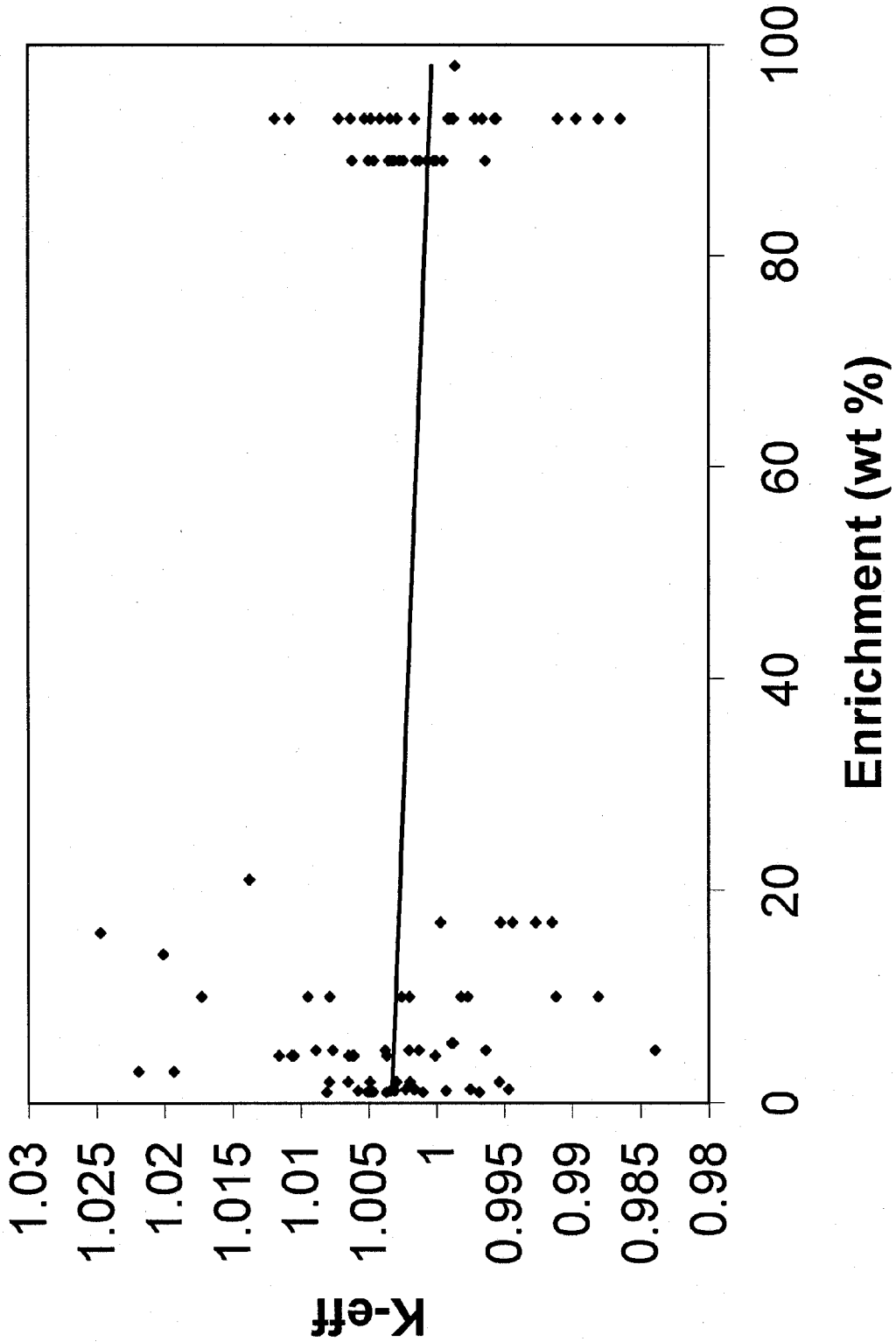

Figure 12 Trend plot for k_{eff} versus enrichment

3.4 Trending Analysis Using D Values

This section will discuss trending analyses using the same set of 102 benchmarks as the traditional analyses shown above; however, the trending parameters are now the D coefficients, described in Volume 1. Even though it is possible to perform the trending on each of the D coefficients independently, it was decided to trend k_{eff} versus the sum of these coefficients (i.e., $D_{sum} = D_c + D_n + D_s$). This combination reduces the number of trends plots to be examined.

The trend plot of k_{eff} versus D_{sum} is given in Figure 13 for the $U(11)O_2$ H/X=3 system.* These plots are analyzed in quite a different method from the traditional approach. Since the D coefficients reflect the deviations of the sensitivities of benchmark systems from the respective sensitivities of the application system, D equal to zero is our goal, i.e., the system does not deviate from itself. A D_{sum} value of zero corresponds to the $U(11)O_2$ H/X = 3 system for Figure 13. The trend line must therefore be extrapolated to zero in order to estimate the Δk bias. Therefore, the slope of the trend line is not nearly as important as where it crosses zero and how many systems are in the region of D_{sum} less than 1.2 (i.e., 3 times 0.4 as postulated earlier). Extrapolation to D = 0 should not be misinterpreted as an extrapolation to systems that are not bracketed between similar systems. From this plot it is clear that perhaps only one other system could be considered similar to the $U(11)O_2$ H/X = 3 system (i.e., D_{sum} less than 1.2). Hence, the predicted bias will have somewhat large uncertainties associated with it. The trend plot for the $U(11)O_2$ H/X = 40 system is shown in Figure 14. Here the coverage near a D_{sum} value of zero is much better than the value shown in Figure 13. In this case, there are at least 8 systems with D_{sum} values of 1.2 or less. The trend plot for the last $U(11)O_2$ system (i.e., H/X = 500) is shown in Figure 15. Here the conclusions are very similar to those in Figure 14. A large number of systems are within a D_{sum} value of 1.2, with a resulting good prediction of the Δk bias for this system.

These trending analysis results are generated using the same software that was used in the traditional trending approach in Section 3.3. Therefore, the same type of estimates for the Δk bias and its uncertainty can be obtained from these analyses. These bias predictions are given in Table 10. Note that the uncertainties in the predicted bias shown in Table 10 all have about the same value. This is due to the use of all benchmarks in the trend for each of these four application systems. An optional choice of using only similar experiments in the trending would have produced biases corresponding closely to the similar experiments, but would have very large (and perhaps invalid) uncertainties for the H/X = 0 and 3 cases due to the very limited number of applicable experiments.

Table 10 Predicted Δk bias and its standard deviation[a] based on D_{sum} trending procedure

Trending Parameters	H/X = 0 System		H/X = 3 System		H/X = 40 System		H/X = 500 System	
	% bias	% std. dev. of biased k_{eff}	% bias	% std. dev. of biased k_{eff}	% bias	% std. dev. of biased k_{eff}	% bias	% std. dev. of biased k_{eff}
D_{sum}	0.74	0.71	1.20	0.70	0.19	0.72	0.09	0.71

[a]Standard deviations correspond to the "pooled standard deviation" as specified in Ref. 5.

*The $U(11)O_2$ H/X = 0 system was analyzed, but the trend plot is not shown. See Table 10 for a summary of the complete results.

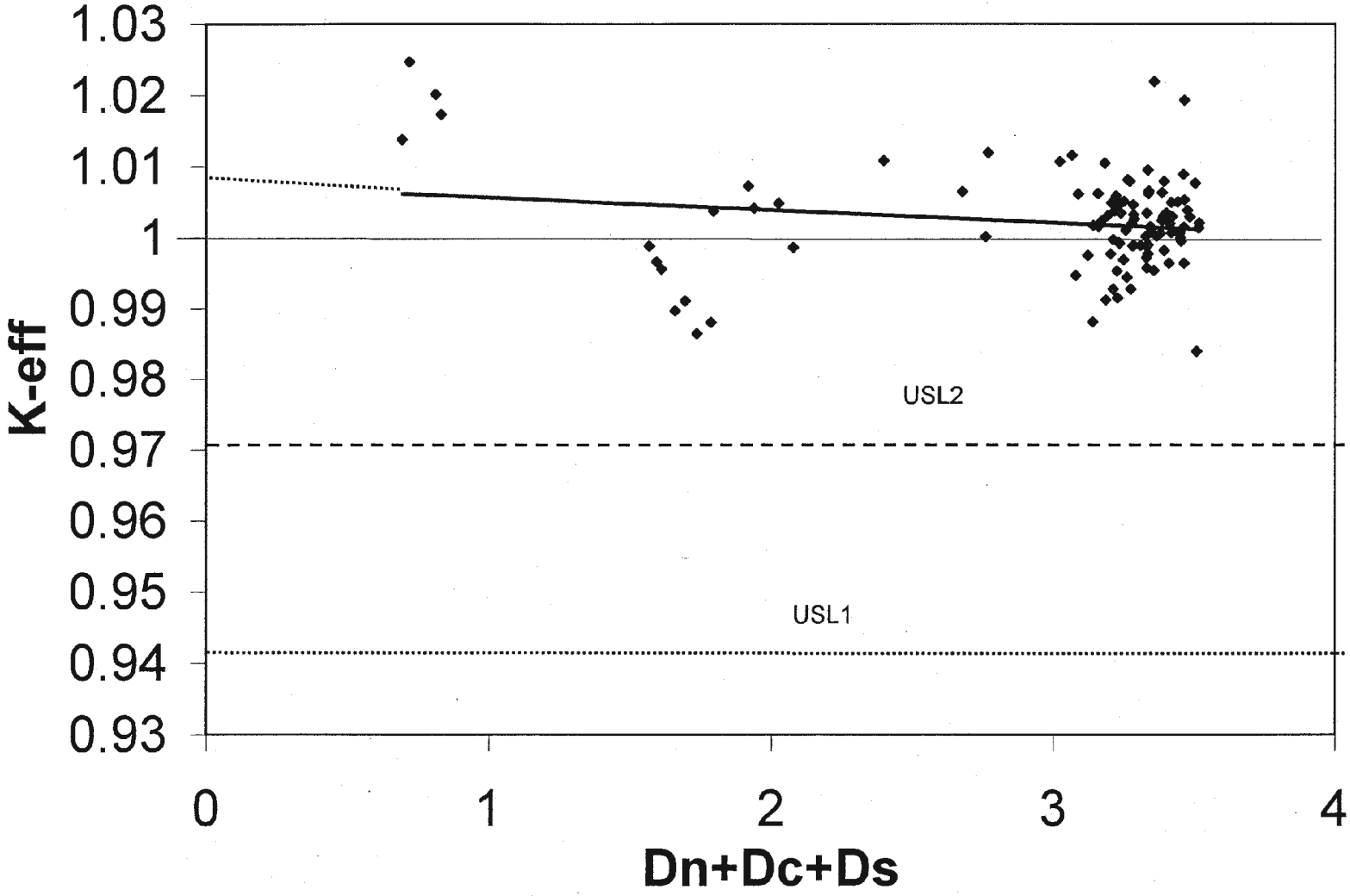

Figure 13 Trend plot for k_{eff} versus D_{sum} value for the $U(11)O_2$ H/X = 3 system

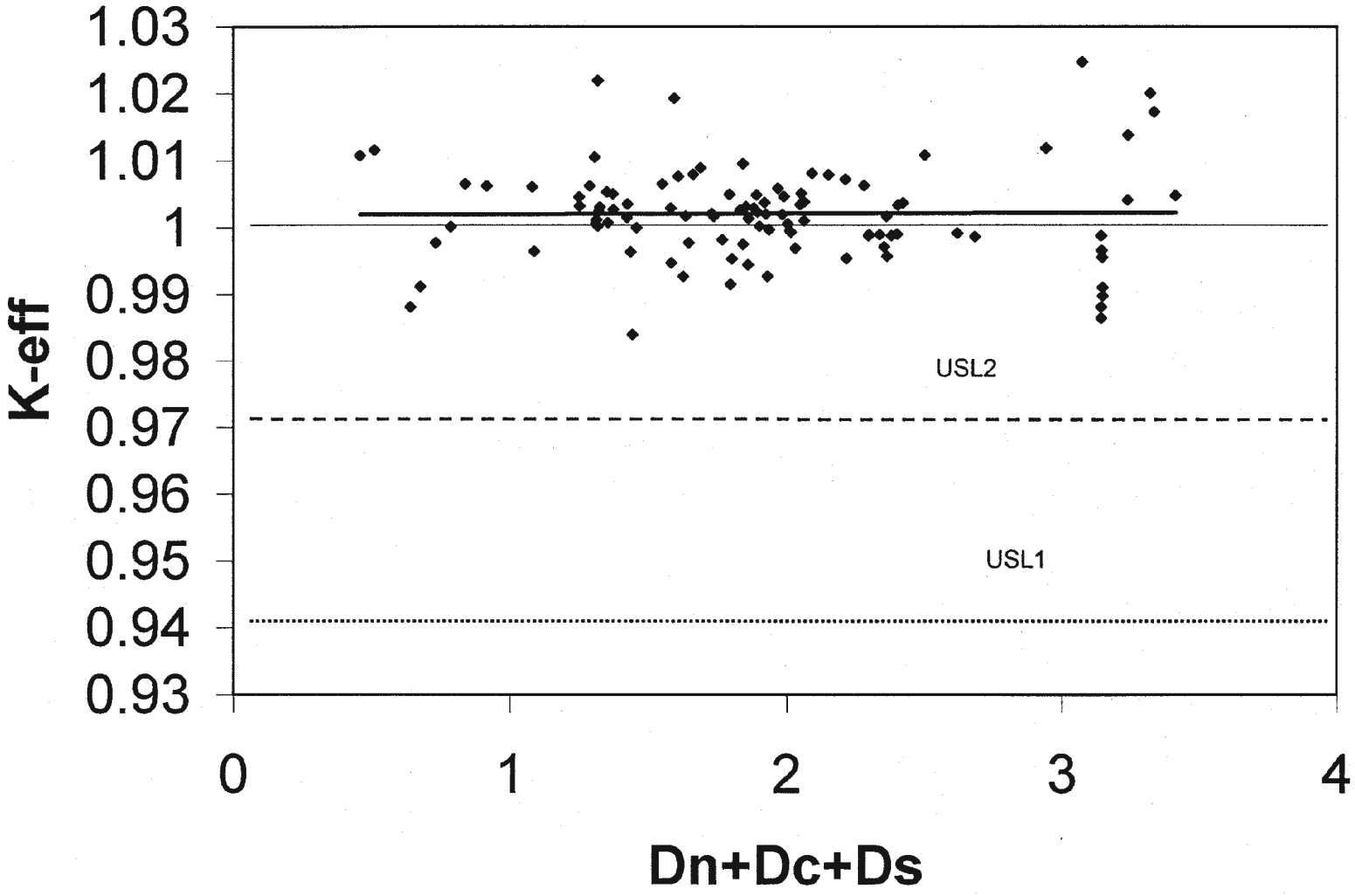

Figure 14 Trend plot for k_{eff} versus D_{sum} value for the $U(11)O_2$ H/X = 40 system

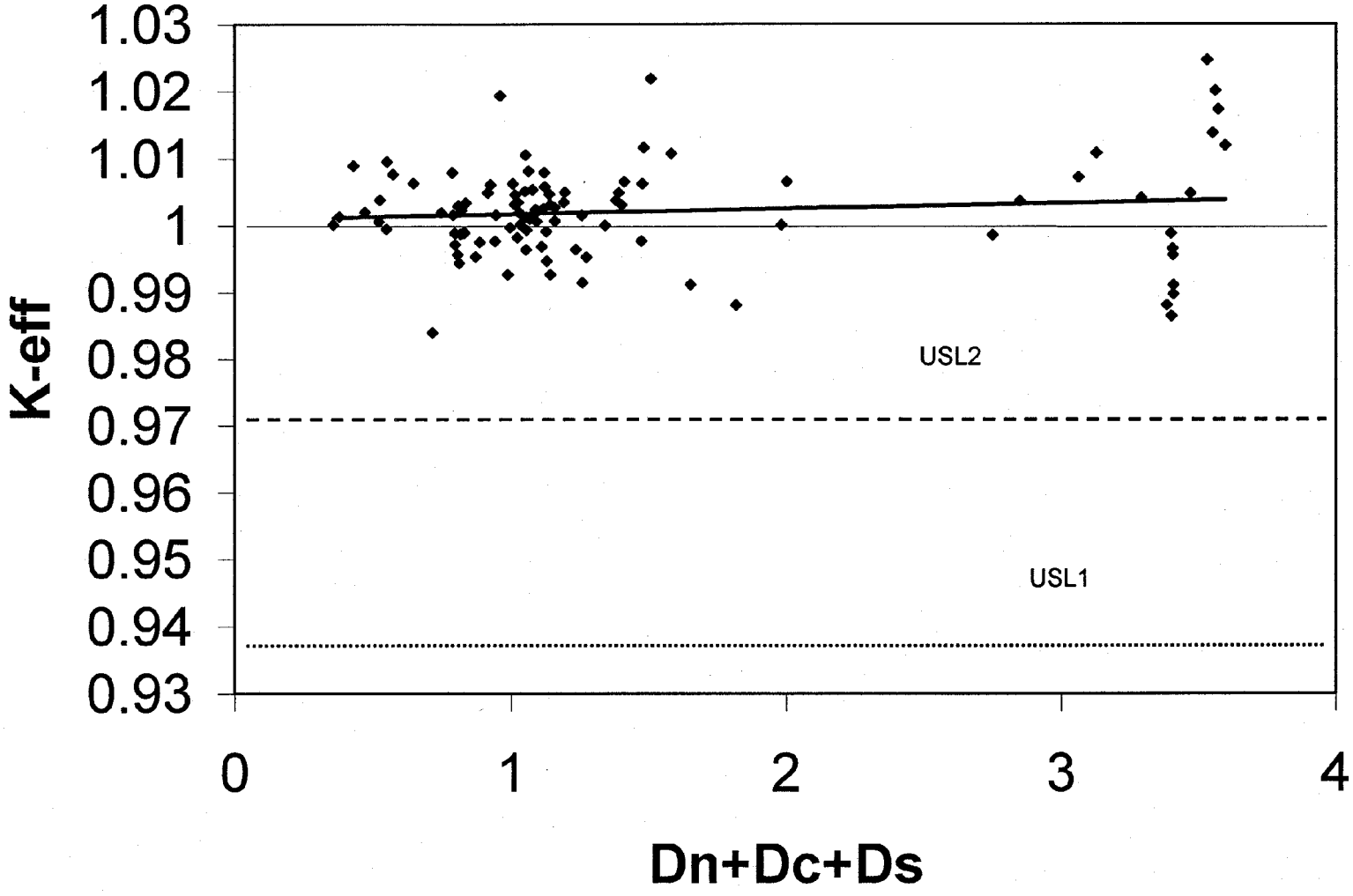

Figure 15 Trend plot for k_{eff} versus D_{sum} value for the $U(11)O_2$ H/X = 500 system

3.5 Trending Analysis Using c_k Values

The trending analyses using the c_k values follow very closely to the analyses using the D coefficients discussed in Section 3.4. Here the trend curves are interpreted as an extrapolation to a c_k value of unity, which corresponds to the particular application system of interest; i.e., correlation coefficient with an experiment identical to the application. The slope of the trend curve is again of secondary importance. The items of primary importance are the number of systems with a c_k value greater than 0.8 and the value of the predicted Δk bias at a c_k value of unity.

The k_{eff} trend plot for c_k of a $U(11)O_2$ H/X = 0 system is shown in Figure 16. This trend plot is interesting when compared with the traditional trend plot shown in Figure 9. The four data points in the upper-right-hand portion of both plots correspond to the same four systems (three ZPR and the Big-10). In Figure 9, the predicted Δk bias is about 0.4% because the overprediction of k_{eff} for these four systems is counteracted by the underprediction of the HEUMET systems, which all have very similar values of EALF. However, the trend seen for k_{eff} in Figure 16 is caused by the lack of similarity between the $U(11)O_2$ H/X = 0 and HEUMET systems. These HEUMET systems have a c_k value of about 0.5–0.6, indicating only minor correlations with the $U(11)O_2$ H/X = 0 system. This example shows the potential improvement from the use of a trending analysis with these new parameters, since trends can be observed as a function of systems that are expressly determined to be similar. It is clear from the preceding analyses that sometimes the traditional parameters indicate that systems should be similar, but are not.

The trend plots for the remaining $U(11)O_2$ systems with H/X values of 3, 40, and 500 are given in Figures 17 to 19. For the system with an H/X value of 3, the predicted biases are higher than those predicted by the standard techniques. The specific reasons for these differences were not explored in depth as with the H/X of 0 cases, but are believed to be caused by the separation of effects that tended to cancel each other. In any case it should be noted that all points with $c_k \geq 0.8$, i.e., similar systems, have k_{eff} values that are greater or equal to one. The Δk bias predicted for the H/X = 40 and H/X = 500 systems are in line with those of the standard techniques since there are a large number of experiments considered to be similar, and no cancellation of effects is seen.

These trending analysis results are generated using the same software that was used previously in Sections 3.3 and 3.4. Estimates of the Δk bias and its uncertainty from this trending approach are given in Table 11. Again, note the similarities of the uncertainties in the bias predictions. This is due to the use of all benchmarks in the trending, regardless of the magnitude of their c_k values.

Table 11 Predicted Δk bias and its standard deviation[a] based on c_k trending procedure

Trending Parameters	H/X = 0 System		H/X = 3 System		H/X = 40 System		H/X = 500 System	
	% bias	% std. dev. of biased k_{eff}	% bias	% std. dev. of biased k_{eff}	% bias	% std. dev. of biased k_{eff}	% bias	% std. dev. of biased k_{eff}
c_k	1.34	0.66	1.15	0.66	0.26	0.72	0.39	0.79

[a]Standard deviations correspond to the "pooled standard deviation" as specified in Ref. 5.

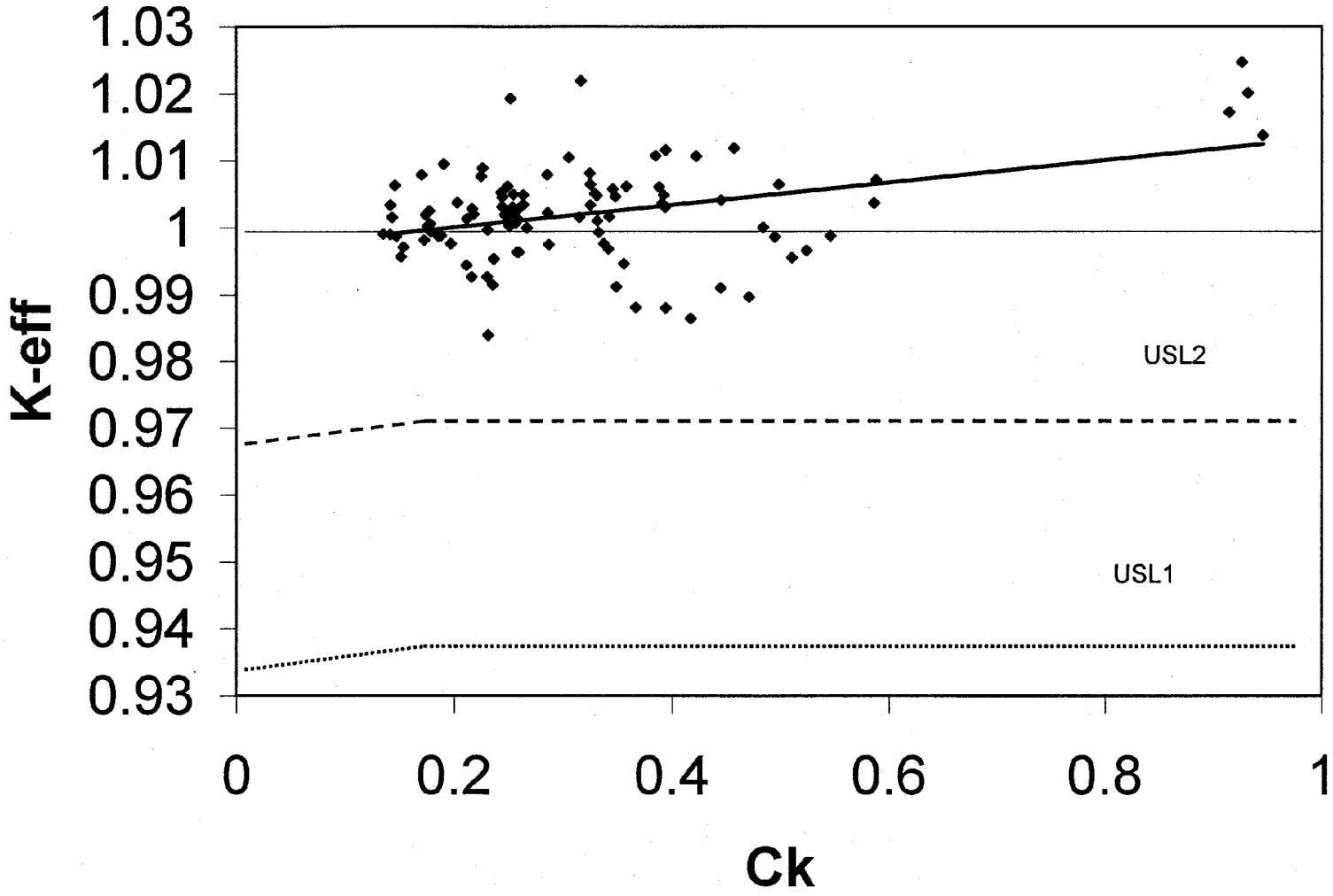

Figure 16 Trend plot for k_{eff} versus c_k value for the $U(11)O_2$ H/X = 0 system

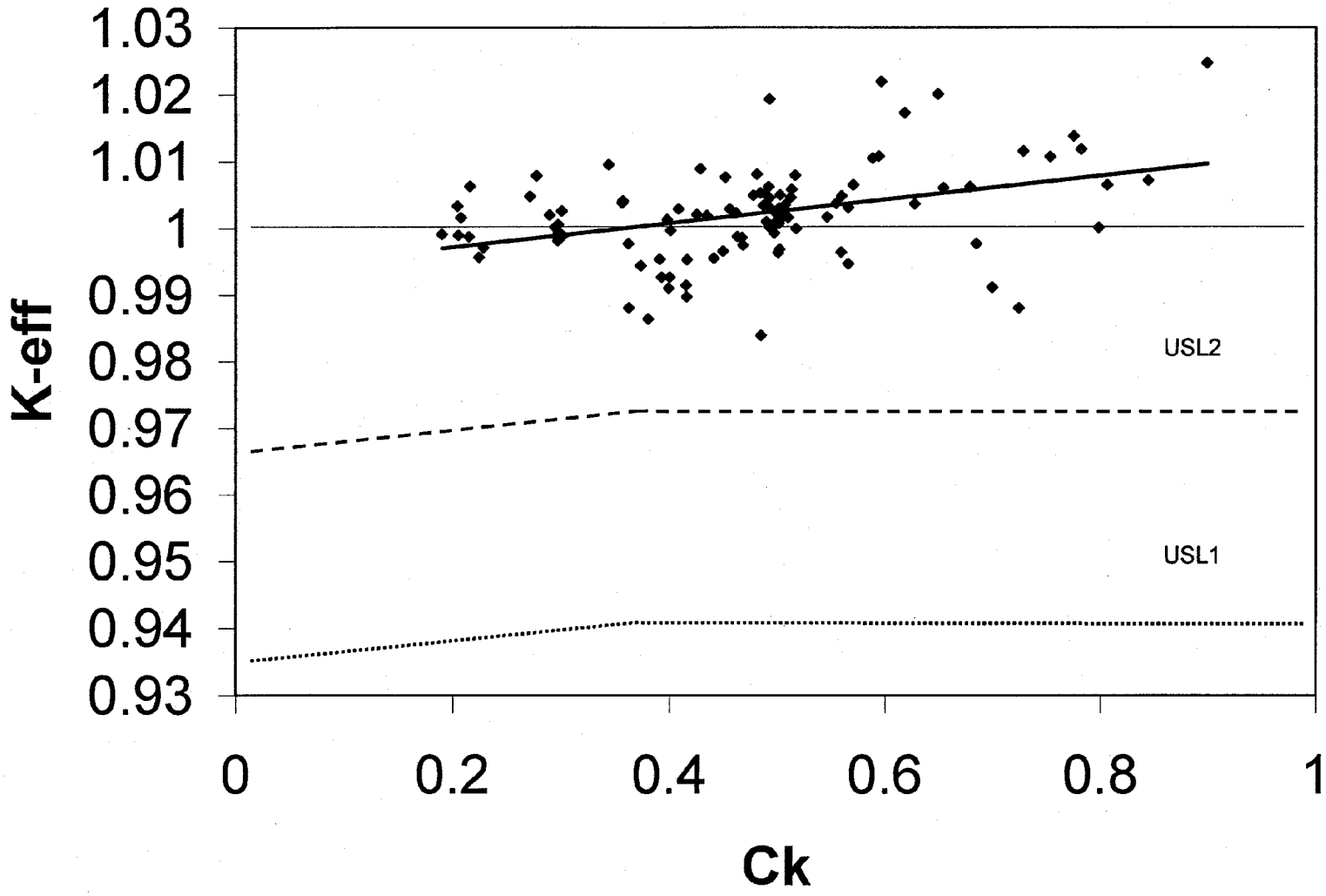

Figure 17 Trend plot for k_{eff} versus c_k value for the $U(11)O_2$ H/X = 3 system

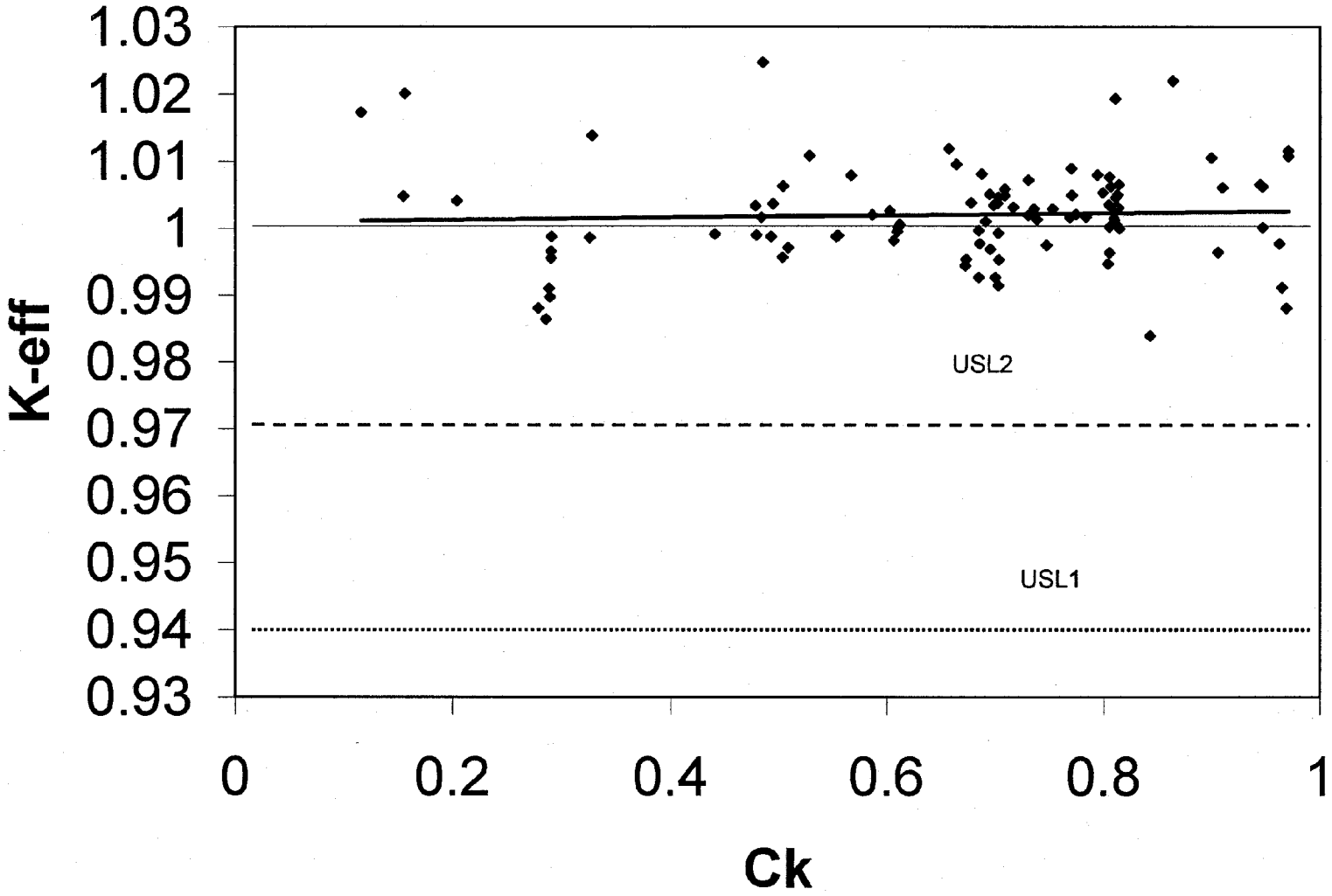

Figure 18 Trend plot for k_{eff} versus c_k value for the $U(11)O_2$ H/X = 40 system

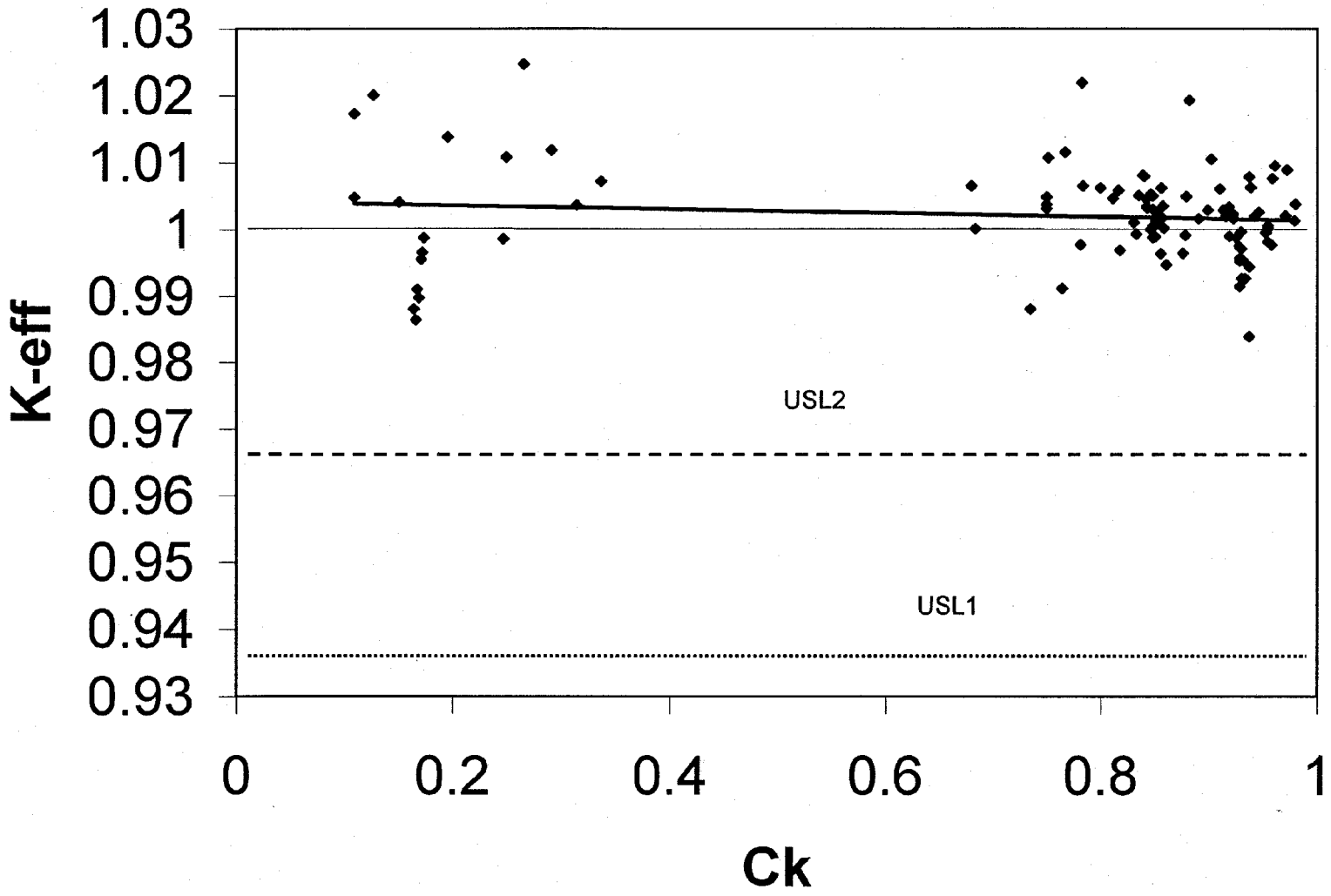

Figure 19 Trend plot for k_{eff} versus c_k value for the $U(11)O_2$ H/X = 500 system

3.6 GLLSM Analysis of 11-wt % Systems

The GLLSM technique is a procedure completely different from the preceding trending techniques, although it does have the same intended endpoint (i.e., the determination of the predicted Δk bias and associated uncertainty for the set of $U(11)O_2$ systems) and GLLSM uses the same sensitivities and correlations as the other techniques. As was shown in Volume 1 of this report, the GLLSM procedure is capable of indicating not only the predicted Δk bias, but also demonstrates its convergence to a single value as the number of experiments is increased. The (e-a)/c quantity used in Figure 20 is the same output value discussed in Volume 1; however, it has a different meaning with regard to an application area as used here. The difference in meaning is due to the lack of an experimental value, e, for an unmeasured application. By convention the calculated and measured values are set to 1.0 for the application, thus (e-a)/c is directly related to $k_a(\alpha) - m_a'$ shown in Eq. (20) in Volume 1, which is the prediction of Δk bias. Shown in Figure 20 is the convergence of the predicted Δk bias as a function of experiment groups. The experimental groups are defined based on similar system characteristics as follows:

Group No.	Experiment descriptions
1	Godiva, HISS, HEUMET
2	ORNL spheres
3	UH3, ORNL L7-L11
4	$U(5)_3O_8$, Big-10, ZPR,
5	SHEBA, Rocky Flats
6	$U(2)F_4$, $U(3)F_4$
7	BAPL, PCTR, TRX
8	Russian experiments

The moderated systems (H/X > 20) appear to converge quicker than the fast systems. In this example, the fast systems require four of the groups to be included for convergence, while the moderated systems only required three groups. This difference is likely due to the larger number of moderated systems, since the procedure does not favor one group of systems over the other. The predicted Δk bias and uncertainties for all 14 of these systems are shown in Table 12.

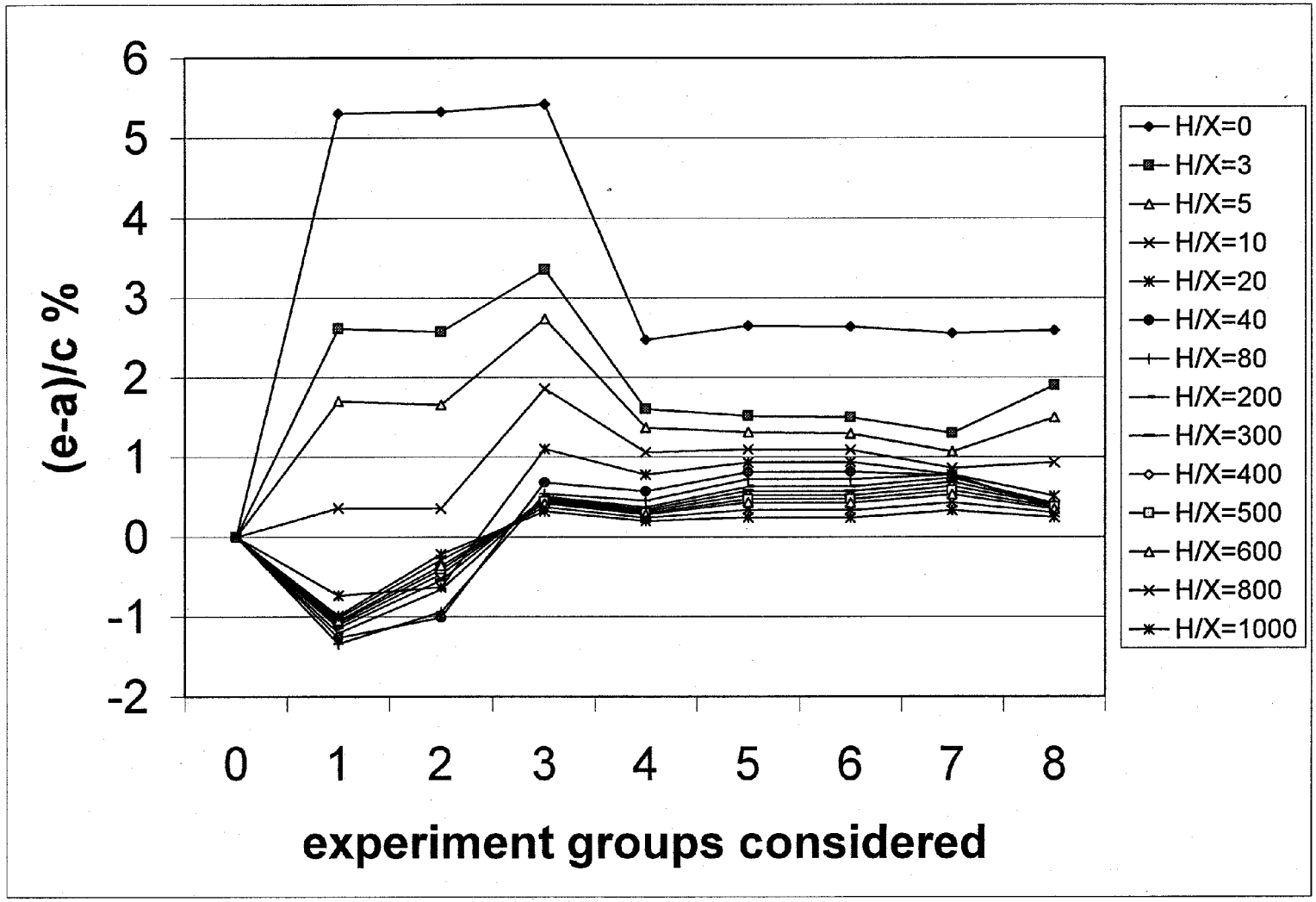

Figure 20 Plot of convergence in predicted k_{eff} bias, [(e-a)/c], for $U(11)O_2$ systems as a function of number of experimental groups considered

Table 12 Predicted Δk bias and its standard deviation[a] based on GLLSM procedure

H/X = 0 System		H/X = 3 System		H/X = 5 System		H/X = 10 System	
% bias	% std. dev. of biased k_{eff}	% bias	% std. dev. of biased k_{eff}	% bias	% std. dev. of biased k_{eff}	% bias	% std. dev. of biased k_{eff}
2.59	0.46	1.90	0.39	1.50	0.35	0.93	0.35

H/X = 20 System		H/X = 40 System		H/X = 80 System		H/X = 200 System	
% bias	% std. dev. of biased k_{eff}	% bias	% std. dev. of biased k_{eff}	% bias	% std. dev. of biased k_{eff}	% bias	% std. dev. of biased k_{eff}
0.51	0.39	0.35	0.43	0.36	0.46	0.42	0.46

H/X = 300 System		H/X = 400 System		H/X = 500 System		H/X = 600 System	
% bias	% std. dev. of biased k_{eff}	% bias	% std. dev. of biased k_{eff}	% bias	% std. dev. of biased k_{eff}	% bias	% std. dev. of biased k_{eff}
0.41	0.42	0.40	0.39	0.37	0.35	0.35	0.33

H/X = 800 System		H/X = 1000 System	
% bias	% std. dev. of biased k_{eff}	% bias	% std. dev. of biased k_{eff}
0.30	0.29	0.24	0.28

[a]Standard deviations correspond to the value output from the GLLSM process. See Appendix B of Volume 1 for details.

3.7 Summary of Trending Analyses

In the preceding sections, results from a number of approaches to criticality safety data validation were presented. Quite interestingly, they give very different answers for the set of application problems chosen for study. The predicted bias are in some cases up to a factor of 15 different. The primary reason for these differences seems to be the inclusion of systems that may "look" very similar from the standpoint of certain parameters, but vary with respect to other parameters. In particular, according to both the H/X and EALF parameters, the HEUMET and ZPR/Big-10 problems are similar. However, with respect to the sensitivities and uncertainties, they appear to be quite different. Cancellation of effects due to systems that "appear" to be similar causes the traditional trending approaches to underpredict the actual bias for low-moderation systems with intermediate enrichments. This situation is evident in Table 13, where each of the previously reported results are presented in summary form. Note also that the differences between the c_k, D, and GLLSM results for low H/X systems would have been minimized if only the similar experiments had been included in the trending studies. The validity for inclusion and the best approach options for inclusion of dissimilar ($c_k < 0.8$ or $D > 1.2$) experiments in the trending analyses will be studied in future work.

Table 13 Comparison of predicted Δk bias and the standard deviation[a] of the estimated k_{eff} for various procedures

Trending Procedures	H/X = 0 System		H/X = 3 System		H/X = 40 System		H/X = 500 System	
	% bias	% std. dev. of biased k_{eff}	% bias	% std. dev. of biased k_{eff}	% bias	% std. dev. of biased k_{eff}	% bias	% std. dev. of biased k_{eff}
EALF	0.17	0.70	0.26	0.70	0.26	0.70	0.26	0.70
H/X	0.32	0.71	0.32	0.71	0.31	0.71	0.17	0.71
D_{sum}	0.74	0.71	1.20	0.70	0.19	0.72	0.09	0.79
c_k	1.34	0.66	1.15	0.66	0.26	0.72	0.39	0.79
GLLSM	2.59	0.46	1.90	0.39	0.35	0.43	0.37	0.35

[a]Standard deviations correspond to the "pooled standard deviation" as specified in Ref. 5.

The predicted bias from these applications are all positive. Since the USLSTATS program[5] sets a positive bias to zero for the purposes of determining USL1 and USL2, the overprediction found in these applications does not present a safety concern. However, a similar situation can be easily postulated where a predicted positive bias is actually a negative bias. With the inclusion of strict confidence levels, along with an additional margin of subcriticality, the cumulative effect of these factors should still be conservative. However, *prudent application of trending procedures is very important in criticality safety validation exercises*.

It can be seen in Table 14 that the predicted USL1 (with an assumed 5% administrative margin of subcriticality for safety) and USL2 values are nearly identical for all the procedures, with the exception of the GLLSM, which predicts USL values some 0.5–1.5% higher due to the lower uncertainty estimates. *Caution is advised with the direct use of the USL values from the GLLSM since these results are estimated based on a comparison of the standard deviations and USL values from the c_k trending analysis.* The development of the statistical basis for the USL values using the GLLSM approach is currently under way in another related project.

Table 14 Comparison of predicted USL1 and USL2 values for the various procedures

Trending Procedures	H/X = 0 System		H/X = 3 System		H/X = 40 System		H/X = 500 System	
	USL1	USL2	USL1	USL2	USL1	USL2	USL1	USL2
EALF	0.938	0.970	0.938	0.970	0.938	0.970	0.938	0.970
H/X	0.937	0.969	0.937	0.969	0.937	0.969	0.937	0.969
D_{sum}	0.937	0.968	0.937	0.967	0.938	0.970	0.938	0.971
c_k	0.938	0.971	0.938	0.971	0.937	0.969	0.936	0.966
GLLSM	0.942	0.979	0.943	0.982	0.942	0.982	0.944	0.985

4 GUIDANCE FOR DETERMINATION OF APPLICABILITY AND ADVANCED TRENDING PROCEDURES

The proposed use of multiple criticality safety data validation techniques is not to make the task of validation more difficult, neither is it to make the task less difficult. The goal of this work is to allow for criticality safety validation under conditions not possible previously, primarily the extrapolation beyond the range of the experimental benchmarks. Techniques developed in this work provide a more rigorous and formal definition of what applicability really connotes.

4.1 Recommendations on the Use of Trending Procedures

As stated in the Volume 1 summary of this document,[6] this work has recommended that two systems with a c_k value of 0.8 or higher can be considered similar enough that one can serve as a benchmark in the validation of the other. This conclusion does not imply that a formal S/U analysis needs to be redone for all previous criticality validation exercises. Clearly, a series of systems with the nearly identical characteristics to the application of interest (i.e., same enrichments, same moderators, a very tightly spaced sequence of moderator/fuel ratio values, similar geometries, etc.,) should be acceptable for use as a validation set. Indeed, in Volume 1 such a series of experiments with constant enrichment was shown to have c_k values greater than 0.9 for H/X values within a factor of 2 of each other.

Thus, the recommendation is that for benchmark data sets that contain more than 20 benchmarks with a c_k value of 0.8 or higher to the corresponding application area, a traditional criticality safety data validation via the standard k_{eff} trending analysis method is acceptable. This recommendation doubles the Volume 1 predicted numbers of benchmarks needed for a reasonable estimate of the k_{eff} bias or the resulting upper subcritical limit. It is further recommended that in using the traditional k_{eff} trending approach that systems with very different characteristics such as high-versus-low enrichment, poisoned-versus-nonpoisoned, wet-versus-dry, etc., not be included together unless that specific effect is being analyzed. For example, do not include three or four random systems with boron poisons in an analysis of nonpoisoned systems. As was seen in the comparison of the traditional-versus-advanced validation procedures in Table 12, the inclusion of widely varying benchmarks can cause cancellation of trends, resulting in an under prediction of the k_{eff} bias. Similar situations could also result in an over prediction of the k_{eff} bias.

The advanced trending analyses, using the D and c_k coefficients as trending parameters, are recommended under conditions that are similar but complimentary to the above recommendations for the traditional trending analyses. The conditions on the advanced trending analyses parameters are as stated in Volume 1 for a meaningful estimate of the k_{eff} bias (i.e., 5–10 experiments with a c_k value of 0.9 or higher or 10–20 experiments with a c_k value of 0.8 or higher). These recommended parameter ranges are only marginally different from those above; however, the motivation for use of these advanced trending analyses is that the inclusion of widely varying system conditions like H/X, enrichment, poisons, etc., are actually encouraged. These advanced techniques are very adept at differentiating between dissimilar systems, while allowing for a wide range of system types to be validated using the single validation data set. To date, the practice has been to include all systems in the benchmark set in the trending analyses; however, future work is planned to explore using only those experiments that are determined to be similar. Applications for which the advanced validation techniques should be applicable are extrapolation scenarios, which are necessary when the desired experiments meeting the strict requirements of the standard techniques are not available. This set of recommended application areas is very well represented by the examples shown in Section 3 for the greater-than-5-wt % enrichment cases.

The final data validation technique presented in this work is the GLLSM methodology. This technique has been extremely useful in the prediction of values of c_k and D that are necessary to define an area of applicability, as well as the determination of the number of experiments needed to obtain a valid estimate of the k_{eff} bias and associated uncertainty. Additionally, this technique can be a useful data validation procedure under practically any set of conditions. However, since the technique is currently much more complex to implement than the other procedures, it is recommended that it only be used in situations where the other approaches are not expected to proceed satisfactorily. The GLLSM technique corresponds to a general validation, where the values of c_k and D fall outside the ranges specified above, or when responses other than k_{eff} are needed for inclusion into the validation. Using the full GLLSM techniques for criticality safety validation can allow for noncritical experiments to be included into the validation procedures. Further development is required before the full GLLSM procedure can be used in these applications, since the "similarity" criteria for the c_k and D parameters may be different when using noncritical systems. A means for ensuring that all important material/reactions and energy regions of a given application problem are tested by the validation procedure must be developed. This procedure would then allow for validation to occur even with a very diverse set of benchmark data (e.g., noncritical measurements).

4.2 Trending Procedures for c_k and D Parameters

The techniques for doing trending analyses with the c_k and D parameters are quite different from those of traditional trending analyses. The traditional analyses allow for multiple systems to be validated from a single trending curve, while the trends with c_k and D parameters only allow a single system per trend plot to be validated. This limitation results from the fact that the trend parameters are only valid between *pairs* of systems. Thus the procedure for doing a trend analysis, with either the c_k or D parameters, is to first generate sensitivity coefficients for all the benchmark problems and all the application scenarios. The application scenarios should cover the range of materials, moderation, enrichment, impurities, etc., that are expected to be used in the criticality safety analyses. If a broad range is needed, it is recommended that the range be broken up into discrete values (like the H/X values in the $U(11)O_2$ example above). A simple postprocessing code should then be able to generate either the c_k or D parameters for all systems. These parameters can then be trended using standard data-fitting codes with the resulting bias and uncertainties of fit and future predictions being extrapolated to either the zero parameter value for D or the unity parameter value for c_k. This trending must be done for each of the application systems that span the range of scenarios for the criticality safety analyses.

The above techniques specify that the sensitivities for all of the benchmark and application systems be quantified. Currently, only 1-D and 2-D geometry capabilities exist for the generation of this sensitivity information; therefore, it is necessary to convert the critical systems into either of these two geometrical systems. Standard procedures are available that make this conversion process easier (cell-weighting, equivalent buckling, etc.), but the conversion can be a time-consuming process that requires some degree of expertise.[8] The development of 3-D sensitivity tools should help alleviate this limitation.

4.3 Guidance on Estimating Experimental Uncertainties

The estimate of an uncertainty matrix can be quite difficult to construct, depending on the availability of a complete description of the experiment. Experimentalists routinely give estimates of the uncertainty in a single experiment, but do not always give enough information to estimate the common uncertainties between a series of critical measurements. If the number of experiments is relatively large, the detailed uncertainty information is typically not

needed. Under these circumstances, it is often desirable to assume that the uncertainties in the respective experiments are uncorrelated and allow for the experimental uncertainties to vary between maximum and minimum quantities. This variation in uncertainties allows a test of the variation in the bias results to be determined. The remainder of this section describes how a full matrix of uncertainties can be generated if sufficient experimental detail is available.

The report describing the $U(2)F_4$ and $U(3)F_4$ experiments[11] estimates the uncertainties in the individual material number densities. The report gives standard deviations in the UF_4 weight percent of 0.7%, paraffin weight percent of 1.2%, enrichment of 1.0% (0.7% for the 3 wt % cases), and density correction of 0.3%. These uncertainty contributions can be used to define a covariance matrix ($\times 10^4$) corresponding to the individual isotopes for the 2 wt % cases as follows:

Material	^{235}U	^{238}U	H	C	F
^{235}U	$0.7^2 + 1.0^2 + 0.3^2$	$0.7^2 + 0.3^2$	0.3^2	0.3^2	$0.7^2 + 0.3^2$
^{238}U	$0.7^2 + 0.3^2$	$0.7^2 + 0.3^2$	0.3^2	0.3^2	$0.7^2 + 0.3^2$
H	0.3^2	0.3^2	$1.2^2 + 0.3^2$	$1.2^2 + 0.3^2$	0.3^2
C	0.3^2	0.3^2	$1.2^2 + 0.3^2$	$1.2^2 + 0.3^2$	0.3^2
F	$0.7^2 + 0.3^2$	$0.7^2 + 0.3^2$	0.3^2	0.3^2	$0.7^2 + 0.3^2$

These covariances can then be combined with the respective sensitivities of k_{eff} to the number densities for each isotope to obtain the uncertainty in k_{eff} due to these effects. The resulting k_{eff} standard deviations for each of the eight experiments are 0.49, 0.45, 0.46, 0.44, 0.42, 0.45, 0.53, 0.52%, respectively. The remaining six experiments for $U(5)_3O_8$ are constructed using the same methods.

4.4 Future Developments

Volume 1 of this report presented the development of S/U and GLLSM techniques for application to criticality safety data validation studies. This volume has applied those methods to the analysis of uranium systems with enrichments greater than 5 wt %. Specifically, a family of $U(11)O_2$ systems with H/X values of 0–1000 have been analyzed. The guidelines given in the previous sections explain when usage of traditional procedures is recommended as well as the situations when the use of these newly developed procedures is recommended. The procedures for using the 1-D sensitivity tool, SEN1, and for trending bias with the resulting D and c_k parameters are established as a result of this development work, however, additional experience with other application areas is required with these new procedures before complete guidance on their use is possible. Work is planned to address the trending with D and c_k values which are outside the proposed similarity criterion of this report. Comparison of trending procedures which exclude experiments which are not similar, include them as shown in this work, and weight them based on their c_k and D values are exercises planned for the future. This experience should allow for development of an upper subcritical limit (USL) procedure that completely takes advantage of these new validation methods. For example, the possibility of a lower administrative margin due to the inclusion of cross section uncertainty effects could be explored.

There are a number of development areas that need further study regarding the use of these techniques. The first area is the need for flexible tools for applying the sensitivity methods to 2-D and 3-D problems. A 2-D capability is currently available,[21] but further work on implementation of a more flexible package is planned. The use of existing inputs for a 3-D Monte Carlo code is considered a must for the routine application of these procedures. Currently work is underway on this task,[24] but further work is needed before this tool will be generally available for use.

The sensitivity methodology applied in this work obtains the sensitivity of k_{eff} to the problem-specific cross sections used in the analysis. Future work is also needed to explore extension of the sensitivity capability to obtain the sensitivity of k_{eff} to the code and data parameters that impact the problem-specific cross section processing. Reference 20 indicates via direct re-calculations how omission of these effects can cause errors in the sensitivity coefficients that are obtained.

The procedures that govern the use of the GLLSM techniques require some additional development before they can be routinely applied in a criticality safety data validation process. These additional developments involve a concept called "completeness," the determination of the rigor involved for data validation versus data evaluation (i.e., self-shielding effects, inclusion of resonance parameter uncertainties, etc), and the addition of non-critical experiment and/or non-k_{eff} response methods.

The completeness concept is needed to ensure that in the general application of GLLSM techniques, where there are no limits for the values of c_k and D, the benchmark data set is complete in the sense that all important reactions and energies are validated. There is a recognized need to investigate and address, as appropriate, the influence and magnitude of shielded and unshielded effects of resonance reactions on the sensitivity and uncertainty analyses relating the GLLSM procedure. The resonance effects include the option of incorporating uncertainties due to self-shielding into the analysis, and also the generation of and processing of resonance parameter uncertainties. The use of non-critical and/or non-k_{eff} responses in the GLLSM analysis is currently available, however, it is not in the SEN1 package that was developed for this project. Either the capability could be added to the SEN1 package or currently available programs that have more complex input requirements could be used. The full use of these capabilities in a 3-D sensitivity generation procedure would simplify the criticality safety validation efforts. Additional measures are also expected to be needed in order for the full GLLSM techniques to be readily used by criticality safety practitioners.

The trending procedures with c_k and the GLLSM applications require the availability of cross section covariance files for processing to a desired group structure. There are currently 27 materials/isotopes with covariance data in ENDF/B-V, and 43 materials/isotopes with covariance data in ENDF/B-VI. However, there are still many important nuclides without covariance information. This information needs to be generated for many isotopes that are of importance to the various criticality application areas.

While the methods and procedures generated as a result of this project are felt to be quite general, they have currently only been applied to uranium systems. Application to other fissile material (e.g., plutonium or mixed oxide) systems is desired to ensure the generality of these procedures. For systems containing primarily uranium fissile materials, the D_{sum} and c_k parameters appear to work equally well. Application to other fissile materials should allow for confirmation of these trends.

5 SUMMARY

This report presents the application of sensitivity and uncertainty (S/U) analysis methodologies developed in Volume 1 to the code/data validation tasks of a criticality safety computational study. Sensitivity and uncertainty analysis methods were first developed for application to fast reactor studies in the 1970s. This work has revitalized and updated the existing S/U computational capabilities such that they can be used as prototypic modules of the SCALE code system, which contains criticality analysis tools currently in use by criticality safety practitioners. After complete development, simplified tools are expected to be released for general use.

The methods for application of S/U and generalized linear-least-squares methodology (GLLSM) tools to the criticality safety validation procedures were described in Volume 1 of this report. Volume 2 of this report presented the application of these procedures to the validation of criticality safety analyses, supporting uranium operations for use in commercial power reactors where the enrichments are greater than 5 wt %.

As a part of this study, a benchmark database of 102 experiments was developed which included not only calculational models and measured-versus-calculational k_{eff} results but also sensitivity and uncertainty results generated by the S/U methodology described in Volume 1. The same tools were then applied to a set of 14 application scenarios corresponding to $U(11)O_2$ systems with H/X values ranging from 0 to 1000. A range of applicability determination was performed using the D and c_k coefficients generated by the S/U analysis. The analysis indicated that the benchmark dataset had good coverage of the 11-wt % systems with H/X values greater than 40, while the systems with H/X less than 40 had only marginal-to-inadequate coverage. The sparsity of low-H/X systems is a concern. Additional experiments in this area would be useful.

Additionally, analyses were performed to predict biases for systems with enrichments greater than 5 wt %. Specifically, the traditional k_{eff} trending analyses were compared with newly developed k_{eff} trending procedures, utilizing the D and c_k coefficients described in Volume 1. Application of these newly developed procedures was made to the family of applications involving $U(11)O_2$ systems with H/X values ranging from 0 to 1000.

The comparisons among the various trending techniques were quite interesting in that they give very different answers, depending on the particular system being analyzed. The predicted biases for various systems were in some cases up to a factor of 5 different between the various trending techniques. The primary reason for these differences was that various systems "look" very similar from the standpoint of certain parameters, but are very different with respect to other parameters. In particular, the H/X and EALF parameters predicted similarity between dry systems with high enrichments (93 wt %) and dry systems with intermediate enrichments (10 wt %), while the c_k and D parameters indicated that these systems were quite different. The net effect of trending with H/X and EALF was a cancellation of effects (the HEU systems were underpredicted by about 1%, the IEU systems were overpredicted by about 2%), which produced a predicted bias of about 0.5% overprediction for a dry $U(11)O_2$ system. The trending with c_k and D parameters produced an estimated bias of between 1 and 2% overprediction since only the IEU systems were predicted to be similar to the dry $U(11)O_2$ system. Although the predicted biases from these applications are all positive, the differences in magnitude are a concern, since the prudent application of trending procedures is very important in criticality validation exercises.

As a result of these observations, the following guidance was developed for usage of the various trending techniques.

- Traditional trending procedures are acceptable for bias estimation if about 10–20 benchmarks with a c_k value of 0.8 or higher are included in the benchmark database. It is further recommended that in using the traditional k_{eff} trending procedures that systems with very different physical characteristics, such as high-versus-low enrichment, poisoned-versus-nonpoisoned, wet-versus-dry, etc., not to be included together unless that specific effect is being analyzed.

- The advanced trending analyses with the D and c_k coefficients are recommended if fewer experiments than those recommended above are available. Also the primary motivation behind their use is that widely varying systems can be included in the analysis, hence making the effective extrapolation of the existing data more meaningful. The procedure will allow for automatic collection of experiments that have similar D and c_k coefficients such that the predicted k_{eff} bias should be valid.

- The GLLSM procedure is recommended if existing experiments with c_k values of 0.8 or higher with respect to the area of application are not available. These experiments, possibly having c_k values 0.2–0.6, are not similar to the application; but they are still relevant. A suite of such experiments can be expected to perform quite well using a GLLSM technique if they are suitably chosen to highlight different aspects of the given application system. Under these conditions, the use of GLLSM for validation is possible, although it may still be desirable to initiate an experimental program to obtain additional data. This procedure also allows for the inclusion of noncritical experiments and non-k_{eff} responses in the validation exercises. Further development is required before these GLLSM techniques can be fully functional in a routine criticality safety validation study.

6 REFERENCES

1. C. R. Weisbin, J. H. Marable, J. L. Lucius, E. M. Oblow, F. R. Mynatt, R. W. Peelle, and F. G. Perey, *Application of FORSS Sensitivity and Uncertainty Methodology to Fast Reactor Benchmark Analysis*, ORNL/TM-5563, Union Carbide Corp., Oak Ridge National Lab., December 1976. See also *Nucl. Sci. Eng.*, **66**, 307 (1978).

2. J. L. Lucius, C. R. Weisbin, J. H. Marable, J. D. Drischler, R. Q. Wright, and J. E. White, *A Users Manual for the FORSS Sensitivity and Uncertainty Analysis Code System*, ORNL-5316, Martin Marietta Energy Systems, Oak Ridge National Lab., January 1981.

3. R. E. Maerker, B. L. Broadhead, and J. J. Wagschal, "Theory of an New Unfolding Procedure in Pressurized Water Reactor Pressure Vessel Dosimetry and Development of an Associated Benchmark Data Base," *Nucl. Sci. Eng.* **91**, 369 (1985). See also *Development and Demonstration of an Advanced Methodology for LWR Dosimetry Applications*, EPRI NP-2188, Electric Power Research Institute, Palo Alto, Calif. (December 1981).

4. N. M. Larson, L. C. Leal, and H. Derrien, *Integral Data Analysis for Resonance Parameters Determination*, ORNL/TM-13495, Lockheed Martin Energy Systems, Inc., Oak Ridge National Lab., September 1997.

5. J. J. Lichtenwalter, S. M. Bowman, M. D. DeHart, and C. M. Hopper, *Criticality Benchmark Guide for Light-Water-Reactor Fuel in Transportation and Storage Packages*, Appendix C, NUREG/CR-6361 (ORNL/TM-13211), U.S. Nuclear Regulatory Commission, Oak Ridge National Lab., March 1997.

6. B. L. Broadhead, C. M. Hopper, R. L. Childs, and C. V. Parks, "Sensitivity and Uncertainty Analyses Applied to Criticality Validation: Volume 1: Methods Development," NUREG/CR-6655, Vol. 1, ORNL/TM-13692/V1, U.S. Nuclear Regulatory Commission, Oak Ridge National Lab., July 1999.

7. *International Handbook of Evaluated Criticality Safety Benchmark Experiments*, NEA/NSC/DOC(95)03/II, Nuclear Energy Agency, Organization for Economic Co-operation and Development, Paris, France (1995).

8. B. T. Rearden, J. J. Lichtenwalter, and C. M. Hopper, *Comparative Results of Reported Critical Experiment Parameters and Uncertainties with First Order Multigroup Perturbation Theory*, NUREG/CR-5624 (ORNL/TM-13718), U.S. Nuclear Regulatory Commission, Oak Ridge National Lab., December 1999.

9. W. C. Jordan, N. F. Landers, and L. M. Petrie, *Validation of KENO V.a Comparison with Critical Experiments*, ORNL/CSD/TN-238, Martin Marietta Energy Systems, Oak Ridge National Lab., December 1986.

10. G. R. Smolen, *Validation Studies Based on Data from Low Concentration Mixed Pu+U Aqueous Critical Experiments*, ORNL-6449, Martin Marietta Energy Systems, Oak Ridge National Lab., August 1988.

11. S. J. Raffety and J. T. Mihalczo, *Homogenized Critical Assemblies of 2 and 3% Enriched Uranium in Paraffin*, Y-DR-14, Union Carbide Corp., Nuclear Division, Oak Ridge Y-12 Plant (1969).

12. D. F. Cronin, *Critical Mass Studies, Part X*, ORNL-2968, Union Carbide Nuclear Corp., Oak Ridge National Lab., 1960.

13. ENDF-202 *Cross-Section Evaluation Working Group Benchmark Specifications*, BNL-19302, Brookhaven National Lab., November 1974.

14. W. C. Jordan and J. C. Turner, *Minimum Mass of Moderator Required for Criticality of Homogeneous Low-Enriched Uranium Systems*, ORNL/CSD/TM-284, Martin Marietta Energy Systems, Inc., Oak Ridge National Lab., December, 1992.

15. Experiments HEU-MET-FAST-003, HEU-MET-FAST-004, and LEU-SOL-THERM-001 in *International Handbook of Evaluated Criticality Safety Benchmark Experiments*, NEA/NSC/DOC(95)03/II, Nuclear Energy Agency, Organization for Economic Co-operation and Development, Paris, France (1995).

16. G. Tuck and I. Oh, *Benchmark Critical Experiments on Low-Enriched Uranium Oxide Systems with H/U = 0.77*, NUREG/CR-0674, U.S. Nuclear Regulatory Commission (1979).

17. R. E. Rothe and G. R Goebel, *Critical Experiments on Low-Enriched Uranium Oxide Systems with H/U = 2.03*, NUREG/CR-2500, RFP-3277, U.S. Nuclear Regulatory Commission (1982).

18. G. A. Linenberger et al., "Enriched-Uranium Hydride Critical Assemblies," *Nucl. Sci. Eng.* **7**, 44 (1960).

19. W. N. Fox et al., "Reactor Physics Measurements on ^{235}U and ^{239}Pu Fuels in an Intermediate Spectrum Assembly," *Journal British Energy Society*, **9** (1970).

20. J. K. Fox et al., *Critical Parameters of Uranium Solutions in Simple Geometry*, ORNL-2609, Oak Ridge National Laboratory, Oak Ridge, Tennessee (1958).

21. R. L. Childs, *SEN1: A One-Dimensional Cross-Section Sensitivity and Uncertainty Module for Criticality Safety Analysis*, NUREG/CR-5719 (ORNL/TM-13738), U.S. Nuclear Regulatory Commission, Oak Ridge National Lab., July 1999.

22. *SCALE: A Modular Code System for Performing Standardized Computer Analyses for Licensing Evaluations*, NUREG/CR-0200, Rev. 5 (ORNL/NUREG/CSD-2/R5), Vols. I–III, March 1997. Available from Radiation Safety Information Computational Center at Oak Ridge National Laboratory as CCC-545.

23. M. D. DeHart and S. M. Bowman, *Validation of the SCALE Broad Structure 44-Group ENDF/B-V Cross-Section Library for Use in Criticality Safety Analyses*, NUREG/CR-6102 (ORNL/TM-12460), U.S. Nuclear Regulatory Commission, Oak Ridge National Lab., September 1994.

24. B. T. Rearden, "Development of SAMS: A Three Dimensional Sensitivity Analysis Module for the SCALE Code System," report of dissertation work, Texas A&M University, December 1999.

INTERNAL DISTRIBUTION

1. S. M. Bowman
2–6. B. L. Broadhead (5)
7–10. W. C. Carter (4)
11. R. L. Childs
12. M. E. Dunn
13. M. D. DeHart
14. K. R. Elam
15. M. B. Emmett
16. I. C. Gauld
17. N. M. Greene
18. G. R. Handley
19. O. W. Hermann
20. D. F. Hollenbach
21–24. C. M. Hopper (4)
25. W. C. Jordan
26. M. A. Kuliasha
27. L. C. Leal
28–32. C. V. Parks (5)
33. L. M. Petrie
34. R. T. Primm
35. C. E. Pugh
36. B. T. Rearden
37. R. C. Robinson
38. R. W. Roussin
39. C. H. Shappert
40. R. G. Taylor
41. T. E. Valentine
42. J. C. Wagner
43. R. M. Westfall
44. R. Q. Wright
45. Central Research Library, Document Reference Section
46. ORNL-Y-12 Technical Library
47–48. ORNL Laboratory Records (2) (for submission to OSTI)
49. ORNL Laboratory Records - RC
50. ORNL Patent Section

EXTERNAL DISTRIBUTION

51. F. M. Alcorn, BWX Technologies, Inc., Naval Nuclear Fuel, 212 Windsor Rd., Lynchburg, VA 24502
52. S. Almodovar, Fluor Daniel Hanford, P.O. Box 1000, Mail Stop A3-02, Richland, WA 99352-1000
53. S. Altschuler, U.S. Department of Energy, Richland Operations, 825 Jadwin, R3-79, Richland, WA 99352
54. R. E. Anderson, Los Alamos National Laboratory, P.O. Box 1663, NIS-6, MS J562, Los Alamos, NM 87545
55. W. L. Andrews, Defense Nuclear Facilities Safety Board, 625 Indiana Ave., Washington, DC 20004
56. C. Apperson, Westinghouse Savannah River Company, Savannah River Site, Bldg. 773-11A, Aiken, SC 29808-0001
57. M. G. Bailey, U.S. Nuclear Regulatory Commission, MS O6-G22, Washington, DC 20555
58. G. H. Bidinger, Nuclear Criticality Safety, 17016 Cashell Road, Rockville, MD 20853

59. R. N. Blomquist, Argonne National Laboratory, RA/208, 9700 S. Case Ave., Argonne, IL 60439-4842
60. C. Boman, BWX Technologies, Inc., Naval Nuclear Fuel, P.O. Box 785, Lynchburg, VA 24505
61. M. C. Brady Raap, Duke Engineering Services, 10503 W. Williams Road, Benton City, WA 99320
62. J. B. Briggs, INEEL, P.O. Box 1625, MS-3855, Idaho Falls, ID 83402
63. T. Burns, Defense Nuclear Facilities Safety Board, 625 Indiana Ave., Washington, DC 20004
64. R. D. Busch, University of New Mexico, Chemical and Nuclear Engineering Department, FEC 209, Albuquerque, NM 87131-1341
65. D. E. Cabrilla, U.S. DOE EM-66, Nuclear Material Stabilization, 19901 Germantown Road, Germantown, MD 20874-1290
66. D. E. Carlson, U.S. Nuclear Regulatory Commission, MS O6-F18, Washington, DC 20555
67. K. J. Carroll, Lockheed Martin Energy Systems, Y-12 Plant, P.O. Box 2009, Oak Ridge, TN 37831-8238
68. P. Cousinou, Institute of Protection and Nuclear Safety, B. P. 6 - 92265 Fontenay-Aux-Roses, Cedex, France
69. D. R. Damon, U.S. Nuclear Regulatory Commission, MS T8-H7, Washington, DC 20555
70. J. R. Davis, U.S. Nuclear Regulatory Commission, MS T8-A33, Washington, DC 20555
71. J. W. Davis, Framatome Cogema Fuels, CRWMS M&O, 1261 Town Center Dr., Las Vegas, NV 89134
72. R. L. Dintaman, U.S. Department of Energy, DP-13, 19901 Germantown Rd., Germantown, MD 20874-1290
73. H. L. Dodds, University of Tennessee, Nuclear Engineering Dept., 214 Pasqua Engineering Bldg., Knoxville, TN 37922
74. T. W. Doering, Framatome Cogema Fuels, 1261 Town Center Drive, Las Vegas, NV 89124
75. F. Eltawila, U.S. Nuclear Regulatory Commission, MS T10-E46, Washington, DC 20555
76. J. D. Evans, U.S. Department of Energy, S-3.1/VISTA, 1000 Independence Ave., S.W., Washington, DC 22085
77. H. D. Felsher, U.S. Nuclear Regulatory Commission, MS T8-H7, Washington, DC 20555
78. P. Felsher, Rocky Flats Environment Technology Site, Bldg. T886B, P.O. Box 464, Golden, CO 80402-0464
79. J. R. Felty, Science Applications Int'l Corp., 2418 N. Dickerson St., Arlington, VA 22207
80. I. E. Fergus, U.S. Department of Energy, EH-22, 20300 Century Blvd., Germantown, MD 20874
81. P. Finck, Argonne National Laboratory, 9700 South Cass Avenue, RA/208, Argonne, IL 60439-4842
82. E. K. Fujita, Argonne National Laboratory, 9700 South Cass Avenue, RA/208, Argonne, IL 60439-4842
83. A. S. Garcia, U.S. Department of Energy, Idaho Operations Office, 850 Energy Dr., MS 1154, Idaho Falls, ID 83401-1563
84. E. Greenspan, University of California, 4101 Etchevenny Hall, Berkeley, CA 94720
85. J. Gulliford, Winfrith Technology Centre, 306/A32, AEA Technology PLC, Winfrith, Dorchester, Dorset DT2 8DH
86. D. K. Hays, Los Alamos National Laboratory, P.O. Box 1663, Los Alamos, NM 87545

87. D. Heinrichs, Lawrence Livermore National Laboratory, P.O. Box 808, MS L-128, Livermore, CA 94551
88. A. B. Hoffman, Lockheed Martin Idaho Tech. Co., P.O. Box 1625, MS 3458, Idaho Falls, ID 83415-3458
89. S. T. Huang, Lawrence Livermore National Laboratory, MS L-128, P.O. Box 808, Livermore, CA 94551
90. J. C. Ingram, Bechtel Jacobs Company LLC, P. O. Box 4699, Bldg. K-1320, MS-7592, Oak Ridge, TN 37831-7592
91. E. F. Kendall, U.S. Department of Energy, Oak Ridge Operations Office, YSO, P.O. Box 2001, Oak Ridge, TN 37831
92. K. D. Kimball, NISYS Corporation, 6055 Atlantic Blvd., Suite G-2, Norcross, GA 30071
93. R. P. Koopman, Lawrence Livermore National Lab., P.O. Box 808, L-467, Livermore, CA 94551
94. M. A. Lee, U.S. Department of Energy, Livermore Operations, 7000 East St., P.O. Box 808, L-293, Livermore, CA 94551-0808
95. R. Libby, Pacific Northwest National Laboratory, P.O. Box 999, M/S K7-74, Richland, WA 99352
96. J. J. Lichtenwalter, Bechtel Jacobs Company LLC, P.O. Box 4699, Bldg. K-1320, MS-7592, Oak Ridge, TN 37831-7592
97. R. C. Little, Los Alamos National Laboratory, MS F663, P.O. Box 1663, Los Alamos, NM 87545
98. C. D. Manning, Siemens Power Corporation, 2101 Horn Rapids Road, P.O. Box 130, Richland, WA 99352-0130
99. R. McBroom, U.S. Department of Energy, Oak Ridge Operations Office, YSO, P.O. Box 2001, Oak Ridge, TN 37831
100. J. McKamy, U.S. Department of Energy, EH-34, 19901 Germantown Road, Germantown, MD 20874-1290
101. R. D. McKnight, Argonne National Laboratory, 9700 S. Cass Ave., Argonne, IL 60439-4842
102. T. P. McLaughlin, Los Alamos National Laboratory, P.O. Box 1663, Los Alamos, NM 87545
103. D. E.I. Mennerdal, E M Systems, Starvãgen 12, Täby, SWEDEN S-18357
104. R. D. Montgomery, Nuclear Fuel Services, Inc., 1205 Banner Hill Rd., Erwin, TN 37650
105. D. C. Morey, U.S. Nuclear Regulatory Commission, MS T8-A33, Washington, DC 20555
106. L. Mantierth, GE Nuclear Energy, P.O. Box 780, Castle Hayne Road, Wilmington, NC 28402
107. J. A. Morman, Argonne National Laboratory, 9700 S. Cass Ave., Bldg. 208, C237B, Argonne, IL 60439-4842
108. R. D. Mosteller, Los Alamos National Laboratory, MS J562, Los Alamos, NM 87545
109. K. A. Niemer, Duke Engineering & Services, 400 S. Tryon St., WC26B, P.O. Box 1004, Charlotte, NC 28201-1004
110. C. W. Nilsen, U.S. Nuclear Regulatory Commission, MS T9-F31, Washington, DC 20555
111. H. Okuno, Japan Atomic Energy Research Institute, 2-4 Shirakara-shirane, Tokai-mura, Ibaraki-ken, JAPAN 319-1195
112. S. A. Parra, Lawrence Livermore National Laboratory, P.O. Box 808, MS L-128, Livermore, CA 94551
113. L. E. Paulson, Manager, Nuclear Safety, GE Nuclear Energy, P.O. Box 780, Castle Hayne Road, Wilmington, NC 28405
114. S. Payne, U.S. DOE/AL/SASD, P.O. Box 5400, Albuquerque, NM 87185-5400

115. V. A. Perin, U.S. Nuclear Regulatory Commission, NMSS/DWM, MS T7-F3, Washington, DC 20555
116. J. Person, Lawrence Livermore National Laboratory, P.O. Box 808, MS L-128, Livermore, CA 94551
117. R. E. Pevey, University of Tennessee, Nuclear Engineering Dept., 214 Pasqua Engineering Bldg., Knoxville, TN 37922
118. J. Philbin, Sandia National Laboratory, P.O. Box 5800, Albuquerque, NM 87185-1143
119. A. W. Prichard, Pacific Northwest National Laboratory, P.O. Box 999, MSIN: K8-34, Richland, WA 99352
120. M. Rahimi, U.S. Nuclear Regulatory Commission, M/S T7F3, Washington, DC 20555
121. T. A. Reilly, Westinghouse Safety Management Solutions, 1993 South Centennial Dr., Aiken, SC 29803
122. J. D. Roarty, Defense Nuclear Facilities Safety Board, 625 Indiana Ave., N.W., Suite 700, Washington, DC 2004
123. C. Rogers, Duke Engineering Services, 10503 W. Williams Road, Benton City, WA 99320
124. C. T. Rombough, CTR Technical Services, Inc., 950 Sugarloaf Rd., Manitou Springs, CO 80829
125. B. Rothleder, U.S. Department of Energy, EH-31, 19901 Germantown Rd., Germantown, MD 20874-1290
126. M. K. Sheaffer, Lawrence Livermore National Laboratory, P.O. Box 808, L-634, Livermore, CA 94550
127. G. L. Stimmell, Manager, General Electric Co., Vallecitos Nuclear Center, P.O. Box 460, Vallecitos Road, Pleasanton, CA 94566
128. J. T. Taylor, Principle Engineer - CSE, GE Nuclear Energy, P.O. Box 780, Castle Hayne Road, Wilmington, NC 28402
129. T. Taylor, Lockheed Martin Idaho Tech. Co., P.O. Box 1625, MS 3458, Idaho Falls, ID 83415-3458
130. D. A. Thomas, Framatome Cogema Fuels, 1261 Town Center Drive, Las Vegas, NV 89124
131. C. Tripp, U.S. Nuclear Regulatory Commission, MS T8-A33, Washington, DC 20555
132. J. A. Thornton, Duke Engineering & Services, 400 S. Tryon St., WC26B, P.O. Box 1004, Charlotte, NC 28201-1004
133. H. Toffer, Fluor Daniel Northwest, Inc., P.O. Box 1050, MSIN B4-44, 1100 Jadwin Ave., Richland, WA 99352-1050
134. E. F. Trumble, Westinghouse Safety Management Solutions, P.O. Box 5388, 1993 South Centennial Dr., Aiken, SC 29803
135. J. J. Wagschal, Racah Institute of Physics, The Hebrew University of Jerusalem, 91904, Jerusalem, ISRAEL
136. M. Wangler, Office of Site Operations, EM-70/CLV-1059, U.S. Department of Energy, 19901 Germantown Road, Germantown, MD 20874-1290
137. L. Wetzel, BWX Technologies, Inc., Naval Nuclear Fuel, P.O. Box 785, Lynchburg, VA 24505
138. S. A. Whaley, U.S. Nuclear Regulatory Commission, MS O6-G22, Washington, DC 20555
139. B. H. White IV, U.S. Nuclear Regulatory Commission, MS O6-F18, Washington, DC 20555
140. D. W. Williams, Westinghouse Electric Corporation, 5801 Bluff Rd MS#15, Columbia, SC 29209
141. Mark Williams, Louisiana State University, Baton Rouge, LA 70803-5820

142. R. E. Wilson, Safe Sites of Colorado, P.O. Box 464, Golden, CO 80402-0464

143. C. J. Withee, U.S. Nuclear Regulatory Commission, MS O6-G22, Washington, DC 20555

NRC FORM 335 (2-89) NRCM 1102 3201, 3202

U.S. NUCLEAR REGULATORY COMMISSION

BIBLIOGRAPHIC DATA SHEET

(See instructions on the reverse)

1. REPORT NUMBER (Assigned by NRC, Add Vol., Supp., Rev., and Addendum Numbers, if any.)

NUREG/CR-6655, Vol. 2
ORNL/TM-13692/V2

2. TITLE AND SUBTITLE

Sensitivity and Uncertainty Analyses Applied to Criticality Safety Validation

Illustrative Applications and Initial Guidance

3. DATE REPORT PUBLISHED

MONTH	YEAR
November	1999

4. FIN OR GRANT NUMBER

W6479

5. AUTHOR(S)

B. L. Broadhead, C. M. Hopper, and C. V. Parks

6. TYPE OF REPORT

Technical

7. PERIOD COVERED ***(Inclusive Dates)***

8. PERFORMING ORGANIZATION — NAME AND ADDRESS ***(If NRC, provide Division, Office or Region, U.S. Nuclear Regulatory Commission, and mailing address; if contractor, provide name and mailing address.)***

Oak Ridge National Laboratory
Post Office Box 2008
Oak Ridge, Tennessee 37831-6370

9. SPONSORING ORGANIZATION — NAME AND ADDRESS ***(If NRC, type "Same as above"; if contractor, provide NRC Division, Office or Region, U.S. Regulatory Commission, and mailing address.)***

Division of Systems Analysis and Regulatory Effectiveness
Office of Nuclear Regulatory Research
U.S. Nuclear Regulatory Commission
Washington, DC 20555-0001

10. SUPPLEMENTARY NOTES

C. W. Nilsen, NRC Project Manager

11. ABSTRACT ***(200 words or less)***

This report presents the application of sensitivity and uncertainty (S/U) analysis methodologies developed in Volume 1 to the code/data validation tasks of a criticality safety computational study. Sensitivity and uncertainty analysis methods were first developed for application to fast reactor studies in the 1970s. This work has revitalized and updated the existing S/U computational capabilities such that they can be used as prototypic modules of the SCALE code system, which contains criticality analysis tools currently in use by criticality safety practitioners. After complete development, simplified tools are expected to be released for general use.

The methods for application of S/U and generalized linear-least squares methodology (GLLSM) tools to the criticality safety validation procedures were described in Volume 1 of this report. Volume 2 of this report presents the application of these procedures to the validation of criticality safety analyses supporting uranium operations where the enrichments are greater than 5 wt %.

12. KEY WORDS/DESCRIPTORS ***(List words or phrases that will assist researchers in locating the report.)***

criticality safety, data validation, sensitivity analysis, uncertainty analysis

13. AVAILABILITY STATEMENT

unlimited

14. SECURITY CLASSIFICATION

(This Page) unclassified

(This Report) unclassified

15. NUMBER OF PAGES

16. PRICE